

## REVIEW ARTICLE OPEN



# A critical review of the application of electromagnetic fields for scaling control in water systems: mechanisms, characterization, and operation

Lu Lin<sup>1</sup>, Wenbin Jiang<sup>1</sup>, Xuesong Xu<sup>1</sup> and Pei Xu<sup>1</sup>✉

Scale deposits in water systems often result in ample technical and economic problems. Conventional chemical treatments for scale control are expensive and may cause health concerns and ecological implications. Non-chemical water treatment technologies such as electromagnetic field (EMF) are attractive options so the use of scale inhibitors, anti-scalants, or other chemical involved processes can be avoided or minimized. Although there are demonstrated beneficial effects of EMF on scale control, the scientific basis for its purported effectiveness is not clear in the available literature, especially lack of quantitative assessment and systematic evaluation of the effectiveness of EMF technologies. This review aims to elucidate the factors pertaining to EMF water treatment and their anti-scaling effects. We have critically reviewed relevant literature on EMF scale control, in particular recent studies, in various water systems, including desalination membranes, heat exchangers (e.g., cooling towers), water pipes, and bulk solutions. We systematically studied the impacts of operational conditions on EMF efficacy, and quantitatively evaluated the EMF improvement on scaling control. The scaling prevention mechanisms, conventional and cutting-edge characterization methods, and potential real-time monitoring techniques are summarized and discussed. The economic benefits of EMF treatment in terms of chemicals, operation and maintenance costs are highlighted. This review provides guidelines for future EMF system design and points out the research needed to further enhance EMF treatment performance.

*npj Clean Water* (2020)3:25; <https://doi.org/10.1038/s41545-020-0071-9>

## INTRODUCTION

Scale deposits in water systems of industrial plants and domestic facilities often cause significant technical problems and economic loss through blocking the flow of water in pipes, reducing efficiency in desalination processes, and decreasing thermal transfer in heat exchangers<sup>1–6</sup>. Commonly encountered scales in water systems are  $\text{CaCO}_3$ ,  $\text{CaSO}_4$ ,  $\text{SrSO}_4$ ,  $\text{BaSO}_4$ ,  $\text{CaF}_2$ ,  $\text{Ca}_3(\text{PO}_4)_2$ , silica, and silicates. Scaling occurs when the concentration of a sparingly soluble salt exceeds its solubility in water. It usually results from changes in pH, temperature, outgassing or pressure that impact the solubility of the salts<sup>7,8</sup>, and a concentration or evaporation process. For instance, when the water temperature increases, the solubility of  $\text{CaCO}_3$  decreases which results in precipitation onto heated surfaces.

The formation of scale is primarily dependent on feed water chemistry. Common types of scale can be categorized into alkaline (e.g.,  $\text{CaCO}_3$ ), non-alkaline (e.g.,  $\text{CaSO}_4$ ), and silica based<sup>9,10</sup>.  $\text{CaCO}_3$  is the most common constituent of scale coming from calcium and bicarbonate ions in surface water, groundwater, brine, and industrial water<sup>11,12</sup>. Other scale forming salts involve a variety of compounds with low solubility in water, such as  $\text{MgCO}_3$ ,  $\text{BaSO}_4$ ,  $\text{Fe}_2(\text{CO}_3)_3$ , iron oxides, silicates, fluorides, and phosphates<sup>7,13</sup>. The common hardness, i.e.,  $\text{CaCO}_3$  crystallizes in three different crystal forms: calcite, aragonite, and vaterite<sup>14,15</sup>. Calcite usually leads to harder scale while aragonite and vaterite form softer scales that are easier to be removed<sup>16–19</sup>.  $\text{CaSO}_4$  and  $\text{Ca}_3(\text{PO}_4)_2$  are common scale constituents in groundwater and wastewater, respectively. Silica and silicates are typically amorphous silicic acid  $[\text{Si}(\text{OH})_4]$  with hydroxide forms of metals, most commonly related to Al, Fe,

Mg, and Ca<sup>20,21</sup>. The silica layer resulting from supersaturation and polymerization of soluble silica is sticky and hard to eliminate<sup>11</sup>.

Scale formation comprises complex phenomena involving supersaturation, nucleation, crystallization, and precipitation<sup>7,22,23</sup>. Crystals generate after supersaturation and nucleation, then grow from solution, but supersaturation is not sufficient for the crystallization of a solution<sup>7</sup>. In other words, the presence of particles, nuclei or seeds in a solution to provide crystallization sites is essential for crystal growth. For example, when  $\text{CaCO}_3$  seeds generate and start to precipitate, other slight solubility salts, like barium and strontium, often co-precipitate with  $\text{CaCO}_3$  even though they have not reached saturation. Nucleation can be initiated through various approaches such as agitation and seeding<sup>24,25</sup>. Scale formation occurs via two crystallization pathways, surface crystallization and bulk crystallization, which are also referred as heterogeneous crystallization and homogeneous crystallization, respectively<sup>7,9,26,27</sup>. Surface/heterogeneous crystallization takes place owing to the lateral growth of the scale seeds entrapped in cavities such as the walls of the vessel containing the solution<sup>7</sup>. Bulk/homogeneous crystallization occurs when crystal seeds form in the bulk phase from the saturated solutions.

In water systems, foreign bodies are referred to water-contacted surface, which can be heat exchangers, water pipes, and membranes. Bulk and surface crystallization may occur individually or simultaneously in all foreign bodies. The formation of scale has caused severe economic losses for these systems. In the case of membrane systems, expenditure due to membrane scaling involves direct costs associated with periodic cleaning, feed water pretreatment, and increased energy demand for membrane scale, as well as indirect costs as a result of reduced water productivity and shortened membrane life<sup>28</sup>. Therefore, various chemical or

<sup>1</sup>Department of Civil Engineering, New Mexico State University, Las Cruces NM 88003, USA. ✉email: pxu@nmsu.edu

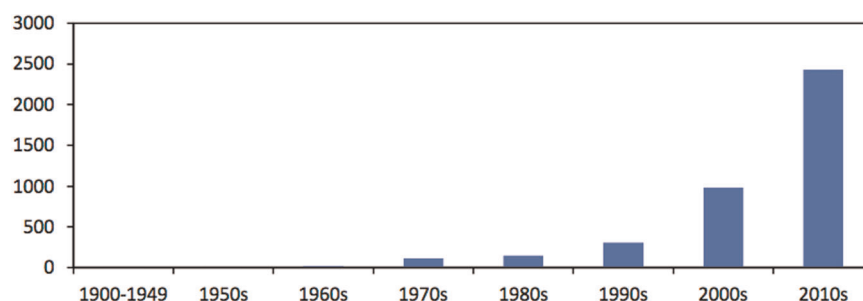


**Fig. 1** Number of publications of EMF associated anti-scaling work. Data collected from Google Scholar.

physical treatments have been used to mitigate scaling. Conventional methods of preventing scale formation include ion exchange, pre-precipitation of the sparingly soluble salts, and addition of chemicals and scale inhibitors. These methods are expensive and may change the solution chemistry, causing health concerns for human or aquatic life<sup>7</sup>. Besides, the scale inhibitors are primarily phosphate compounds, which may be harmful to the environment bringing about undesired effects such as eutrophication and algal blooms.

Examples of non-chemical water treatment systems include electromagnetic field (EMF), ultrasonic, catalytic materials, and alloys<sup>11,29–31</sup>. Ultrasonic wave can bring significant mechanical and thermal effects, generate powerful shock wave and microstreaming to prevent scaling<sup>32</sup>. Trace amount of catalytic materials like Zn can slow down the nucleation rate of calcium carbonate and also promote its crystallization in the aragonite rather than calcite form<sup>30</sup>. EMF as a scale control device has been employed for over a century<sup>33–35</sup>. The use of EMF as non-chemical water treatment devices for scale control was initially proposed by Porter<sup>36</sup>. Faunce and Cabell<sup>37</sup> invented an electromagnetic device to treat boiler feed water. In 1873, Hay received the first US patent for an EMF water treatment device<sup>38</sup>. Baker and Judd<sup>8</sup> reviewed industrial applications of commercial EMF devices from last century and assessed the proposed mechanisms for EMF. Salman et al.<sup>39</sup> outlined successful and unsuccessful studies of anti-scaling effects of EMF, but lacked the synergistic analysis of these cases. Ambashta and Sillanpää<sup>40</sup> described water purification technique using magnetic assistance and explained different aspects of magnetism and magnetic materials for water purification. Piyadasa et al.<sup>11</sup> summarized the relevant literature on the problem of scaling and biofouling in reverse osmosis (RO) membranes and heat exchanger systems, with a particular focus on pulsed-EMF treatment. A recent review by Alabi et al.<sup>7</sup> discussed the possible mechanisms and observed effects implicated to EMF water treatment.

EMF has a long and controversial history regarding its anti-scaling effectiveness in water systems although it has reportedly proven effective for numerous industrial applications<sup>41</sup>. Over 4,000 studies have reported EMF associated anti-scaling and anti-fouling work from last century, and the quantity of publications increased exponentially during this century (Fig. 1), indicating EMF is a critical technique for scaling control. In these publications, EMF has been applied to mitigate bacterial contamination, organic, and inorganic fouling; improve oil separation and water splitting; assist other water treatment technologies, e.g. electrocoagulation, advanced oxidation processes. However, up to date, it has not been fully scientifically demonstrated that the EMF exposure is powerful enough to produce strong anti-scaling effects, and the various effects and mechanisms remain unclear. The inconsistency of EMF studies possibly attributes to the use of non-standardized methods, variations in water composition or differences in the course of the operations<sup>11</sup>. The efficiency of magnetic water treatment could also depend on the nature of the pipe materials<sup>1</sup>. In many cases, the standardized operating procedures are often

ambiguous and important parameters including pipe materials, exposure time and properties of the field, are only partly reported. No general consensus has been reached regarding the effect of these variations on the application of EMF.

The a priori scientific understanding is needed to investigate the mechanisms of EMF and the factors affecting the effectiveness of the technologies. Thus, we conducted an extensive literature review on EMF applications and focused on the impacts of operating conditions on anti-scaling efficacy in water systems. The EMF treatment discussed in the present review includes electric field, magnetic field, and EMF, which are collectively called EMF in this review. The treatment refers to passing water through an EMF of certain characteristics. EMF devices can be placed on the treated water prior to entering the water systems, or in the position of scaling surface, referred as pretreatment and co-treatment, respectively. The possible scaling prevention mechanisms, characterization methods, factors pertaining to EMF water treatment, and the economics of the anti-scaling effects, are discussed herein.

## SUMMARY OF RECENT EMF TREATMENT STUDIES

Among a substantial number of literatures, 48 studies with detailed experiment methods and results (published after the year 2000) were selected for in-depth analysis. Tables 1–4 summarize the details of these studies including the feed water solution, EMF devices and treatment, testing conditions (laboratory, pilot, or industrial-scale) and duration, materials and operating conditions, characterization methods, and major results. Although different results were reported regarding the influence of EMF in minerals precipitation, the results support the same hypothesis that EMF induce bulk precipitation of crystals rather than adhesion to the surface of reactors, pipes and vessels (Tables 1–3) or to membrane surface (Table 4). If we consider the bulk precipitation enhancement as effective EMF treatment, the percentage of effective EMF cases can reach 95% for the discussed 48 studies, 5% of the studies observed negligible improvement with EMF treatment, none of them has negative results. Negligible improvement with EMF was observed due to feed water chemistry or high water recovery, more details were discussed in section “RO System Operation & Water Chemistry”. It is also worth noting that many studies fail to report negative results, thereby the percentage of successful cases could be lower in reality.

### EMF treatment on bulk solutions, reactors and pipes

As shown in Tables 1–3, almost all EMF treatments on bulk solution, reactors and pipes are effective (97.6%). The study by Lipus and Dobersek<sup>42</sup> with EMF treatment on heat exchange surfaces concluded that fine-suspended particles formed in the bulk solution were washed away by water flow. EMF was also reported to alter the precipitation of  $\text{CaCO}_3$  from forming surface nucleating scale to non-adherent bulk solution particles<sup>43</sup>. Similar results were obtained by Alimi et al.<sup>44</sup> that EMF affected  $\text{CaCO}_3$

**Table 1.** Summary of recent EMF water treatment studies on heat exchangers.

| Solution  | Characterization                                       | EMF/Treatment  | Set-up                                     | EMF anti-scaling effect  | Ref.   |
|---|--|--|--|--|--------|
| Tap water: $Mg^{2+}$ and $Fe^{2+}$ , calcite, aragonite   | • XRD<br>• SEM   | • 0.6 and 0.8 V s/m <sup>2</sup><br>• Permanent magnets<br>• Pretreatment      | Lab-scale                                  | • EMF formed 70% sediment and thinner aragonite crystals compared to non-treatment<br>• Fine-suspended particles formed and washed away by water flow  | 41     |
| Tap water   | • TEM<br>• EDX   | • 0.5–1.3 T<br>• Permanent magnets   | Pilot plant 2 years                        | • Soft aragonite nucleated and grew with EMF > 0.5 T<br>• EMF reduced 70% precipitation<br>• A slightly higher weight gained with EMF than chemical treatment  | 17     |
| Aggregating a commercial Ludox silica sol with 36 nm primary particle size aggregated using $KNO_3$ solution to a size of 1400 nm   | • PSD  | • 0.31 T<br>• Permanent magnets<br><i>NdFeB block magnet</i><br>• Pretreatment | Lab-scale                                  | • EMF was efficient to disperse nanoparticles and intensify the dispersion process, especially under turbulent flow<br>• The de-aggregation effect was a combination of hydrodynamic forces and Lorentz forces   | 78     |
| Lake water: $Ca^{2+}$ 63 mg/L, $Mg^{2+}$ 27 mg/L, $SO_4^{2-}$ 37 mg/L, no free $CO_2$ , pH = 8.3, TH 272 mg/L as $CaCO_3$ , CH 260 mg/L as $CaCO_3$ , TSS 14.7 mg/L, $SiO_2$ 10 mg/L, TSR 356 mg/L  | • XRD<br>• PIXE  | • Permanent magnets<br>• Co-treatment  | Large-scale 4 months                       | • EMF generated amorphous, soft deposit of silica hydrosol<br>• Crystallization of calcite was blocked due to strong adsorption of $Ca^{2+}$ and other metal ions on magnetically activated silica<br>• A small amount of silica in water was necessary for EMF to prevent the system against lime scale | 111    |
| $Ca^{2+}$ 107 mg/L, $Mg^{2+}$ 46 mg/L, $Na^+$ 134 mg/L, $K^+$ 17 mg/L, $Fe^{2+}$ 1.5 mg/L, $SO_4^{2-}$ 354 mg/L $Cl^-$ 96 mg/L, $SiO_2$ 12 mg/L, free $CO_2$ 22 mg/L, pH = 8.0, CH 265 mg/L as $CaCO_3$ , TH 458 mg/L as $CaCO_3$ , TSS 17.4 mg/L, TSR 987 mg/L | • XRD<br>• SEM<br>• FT-IR                              | • Permanent magnets<br>• Co-treatment  | 1 GW power plant                           | • No scale cake generated for several months after EMF installed<br>• A small amount of soft and loose deposit was recovered   | 111    |
| pH 7.15, $Ca^{2+}$ 318 mg/L, TH 540 mg/L as $CaCO_3$ , TDS 690 mg/L   | • SEM<br>• $Ca^{2+}$ concentration<br>• Scaling weight | • Solenoid coils<br>• Pretreatment   | Lab-scale 1.6 cm×10 cm copper pipe 0.5 m/s | • EMF improved heat transfer efficiency<br>• The increasing water velocity decreased EMF efficiency  | 109    |
| Electrical conductivity 2,000 and 4,000 $\mu S/cm$  | • SEM  | • 0.16 T<br>• Solenoid coils<br>• Pretreatment                                 | 820 h 5 ft high cooling tower              | • EMF altered the precipitation of $CaCO_3$ from a surface nucleating scale to a non-adherent bulk solution powder<br>• A 20- $\mu m$ filter maintain zero fouling resistance over 820 h in a concentric tube heat exchanger   | 42     |
| $Ca^{2+}$ 200 mg/L, $HCO_3^-$ 610 mg/L  | • SEM<br>• PSD   | • Solenoid coils<br>• Pretreatment   | Lab-scale 50 L                             | • EMF improved heat transfer efficiency<br>• EMF altered the $CaCO_3$ crystal phase from aragonite to calcite<br>• EMF accelerated particle growth   | 16,126 |
| Conductivity 1,200 $\mu S/cm$   | • Conductivity<br>• PSD<br>• SEM                       | • 0–100 V, 0–400 kHz<br>• Solenoid coils<br>• Pretreatment                     | Lab-scale 40 L                             | • EMF decreased conductivities by 17–25% with different frequencies, whereas the untreated case dropped by 31%<br>• The $CaCO_3$ particle size became smaller and the crystals were loose with EMF   | 127    |
| $CaCl_2$ 829 mg/L, $NaHCO_3$ 573 mg/L   | • SEM-EDS<br>• XRD                                     | • Combined electrostatic and pulsed EMF<br>• Pretreatment                      | Lab-scale                                  | • With EMF, the particle size of scale became smaller and the morphology became loose<br>• EMF effect favored aragonite and restrained calcite   | 128    |

**Table 1** continued

| Solution   | Characterization   | EMF/Treatment  | Set-up    | EMF anti-scaling effect  | Ref.           |
|--|--|--|-----------|--|----------------|
| Brine solutions: $\text{Ca}^{2+}$ 110–8200 mg/L, $\text{HCO}_3^-$ 150–700 mg/L   | <ul style="list-style-type: none"> <li>Conductivity</li> <li>pH</li> <li>Pressure</li> </ul>                           | <ul style="list-style-type: none"> <li>0.65–1.35 T</li> <li>Permanent magnet</li> <li>Neodymium N45SH</li> <li>Pretreatment</li> </ul> | Lab-scale | <ul style="list-style-type: none"> <li>Bicarbonate played a key role in EMF treatment for anti-scaling</li> <li>Laminar flow was required for separation of charged particles by EMF</li> <li>EMF could impact the structure of the ionic species</li> </ul>   | <sup>129</sup> |
| Synthetic hard water with hardness 500 mg/L  | <ul style="list-style-type: none"> <li>Deposited weight</li> <li>SEM</li> <li>PT100 resistance thermometers</li> </ul> | <ul style="list-style-type: none"> <li>0–4000 V</li> <li>Permanent magnet</li> <li>Pretreatment</li> </ul>                             | Lab-scale | <ul style="list-style-type: none"> <li>500 V was the optimal to reduce 52.8% fouling resistance and 61.3% deposited weight</li> <li>The structure of <math>\text{CaCO}_3</math> changed from aragonites to spherical vaterites as voltage increased</li> </ul> | <sup>130</sup> |
| XRD X-ray diffraction, SEM scanning electron microscopy, TEM transmission electron microscopy, EDX energy dispersive X-ray spectroscopy, PIXE proton induced X-ray emission, FT-IR Fourier-transform infrared spectroscopy, TH total hardness, CH carbonate hardness, TS total suspended solids, TSS total solid residue, TDS total dissolve solids, PSD particle size distribution, T tesla (unit). |  |  |           |  |                |

**Table 2.** Summary of recent EMF water treatment studies on pipes and other substrates.

| Solution   | Characterization  | EMF/Treatment  | Set-up  | EMF anti-scaling effect   | Ref.           |
|--|---|--|---|---|----------------|
| 400 mg/L $\text{CaCO}_3$   | <ul style="list-style-type: none"> <li>Weight precipitates.</li> <li><math>\text{Ca}^{2+}</math> concentration</li> </ul> | <ul style="list-style-type: none"> <li>0.16 T.</li> <li>Permanent magnets.</li> <li>Co-treatment.</li> <li>Pretreatment</li> </ul> | Lab-scale PTFE, Tygon, PVC, copper, and stainless-steel pipes 0.5 L   | <ul style="list-style-type: none"> <li>EMF increased the total precipitate quantity and favored its formation in bulk solution instead of walls.</li> <li>Pipe material was critical for EMF; non-conductive materials were the most efficient.</li> <li>Roughness of the wall had negligible effect</li> </ul> | <sup>43</sup>  |
| 500 mg/L $\text{CaCO}_3$   | <ul style="list-style-type: none"> <li><math>\text{Ca}^{2+}</math> concentration</li> </ul>                               | <ul style="list-style-type: none"> <li>0.16 T.</li> <li>Home-made Permanent magnets.</li> <li>Pretreatment</li> </ul>              | Lab-scale PVC, copper, and stainless steel                            | <ul style="list-style-type: none"> <li>The increasing EMF treatment time had negligible effect.</li> <li>EMF was more efficient in stainless steel and copper than PVC.</li> </ul>  | <sup>1</sup>   |
| $\text{Ca}(\text{HCO}_3)_2$  | <ul style="list-style-type: none"> <li>XRD.</li> <li>TEM.</li> <li>EDX</li> </ul>   | <ul style="list-style-type: none"> <li>1.2 T</li> </ul>  | Lab-scale Stainless-steel pipe  | <ul style="list-style-type: none"> <li>There was a maximum efficiency at an optimal flow rate</li> <li>EMF favored the formation of aragonite than calcite</li> </ul>   | <sup>131</sup> |
| Slurries of marble, limestone, gypsum, dolomite, tricalcium phosphate, and low-grade phosphate rock  | <ul style="list-style-type: none"> <li>Cumulative weight</li> </ul>   | <ul style="list-style-type: none"> <li>0.2 T.</li> <li>Permanent magnets.</li> <li>Pretreatment</li> </ul>                         | Lab-scale PVC pipe  | <ul style="list-style-type: none"> <li>EMF enhanced solubility of four calcium compounds: 25% (limestone), 14.7 % (calcite), 4.9% (gypsum), 0.92% (dolomite), and 64% (tricalcium phosphate)</li> </ul>   | <sup>132</sup> |
| 0.89 mg/L $\text{CaCl}_2$ and 0.85 mg/L $\text{Na}_2\text{CO}_3$   | <ul style="list-style-type: none"> <li>Flame photometer for deposit amount.</li> <li>XRD</li> </ul>                       | <ul style="list-style-type: none"> <li>0.1 T.</li> <li>Permanent magnets</li> </ul>  | Lab-scale Stainless steel, copper, aluminum, and glass substrates 4 L | <ul style="list-style-type: none"> <li>Deposits decreased with increasing temperature.</li> <li>For the tests at 20–80 °C, the largest EMF effect was 50% reduction of the deposit on glass at 60 °C</li> </ul>   | <sup>115</sup> |
| 10.6 g/L $\text{Na}_2\text{CO}_3$ and 11.1 g/L $\text{CaCl}_2$   | <ul style="list-style-type: none"> <li>Titration.</li> <li>XRD</li> </ul>   | <ul style="list-style-type: none"> <li>0.1–0.3 T.</li> <li>Permanent magnets.</li> <li>MagneGen.</li> <li>Co-treatment</li> </ul>  | Lab-scale fluidized-bed crystallizer                                  | <ul style="list-style-type: none"> <li>Higher EMF intensity yielded a lower calcite growth rate.</li> <li>EMF suppression was higher at low levels of supersaturation, pH, and ionic strength</li> </ul>  | <sup>99</sup>  |
| PVC polyvinyl chloride, PTFE polytetrafluoroethylene, XRD X-ray diffraction, EDX energy dispersive X-ray spectroscopy, TEM transmission electron microscopy, T tesla (unit). |   |  |   |   |                |

**Table 3.** Summary of recent EMF water treatment studies on bulk solutions.

| Solution  | Characterization  | EMF/Treatment   | Set-up               | EMF anti-scaling effect  | Ref. |
|---|---|---|----------------------|--|------|
| Potable water: TH 373 mg/L as $\text{CaCO}_3$ , $\text{Ca}^{2+}$ 117 mg/L, $\text{Mg}^{2+}$ 14.7 mg/L.  | • PSD   | • 0.33 T<br>• Permanent magnets.<br>• <i>NdFeB block magnet</i><br>• Pretreatment   | Lab-scale            | • Suspended particles could be fragmented by EMF at a turbulent flow<br>• No effect of de-aggregation under laminar regime<br>• Turbulent flow conditions were required for effective EMF  | 44   |
| Heating water containing 120 mg/L $\text{Ca}^{2+}$  | • XRD<br>• SEM  | • 0.1 T<br>• Teflon-coated ferrite ring magnets<br>• <i>D-fluid, Milan</i>  | Lab-scale            | • EMF produced aragonite rather than calcite<br>• The treatment effect persisted for over 200 h after EMF terminated   | 19   |
| Hard water: 1,215 mg/L $\text{Ca}(\text{HCO}_3)_2$  | • XRD<br>• TEM<br>• EDX                                   | • 0.5–1.3 T<br>• Permanent magnets<br>• Newport Instruments   | Lab-scale<br>100 mL  | • EMF favored aragonite<br>• Magnetic induction and exposure time could affect aragonite content; the fluid velocity had no impact<br>• EMF has little influence on zeta potential of precipitates   | 18   |
| $\text{Ca}^{2+}$ 33 mg/L, $\text{Mg}^{2+}$ 6.5 mg/L, $\text{Na}^+$ 1.9 mg/L, $\text{K}^+$ 0.6 mg/L, $\text{Si}^{2+}$ 0.16 mg/L, $\text{HCO}_3^-$ 128 mg/L, $\text{SO}_4^{2-}$ 11.6 mg/L, $\text{NO}_3^-$ 2.4 mg/L, $\text{Cl}^-$ 1.7 mg/L<br>$\text{Ca}^{2+}$ , $\text{CO}_3^{2-}$ , and $\text{HCO}_3^-$ , 300–500 mg/L as $\text{CaCO}_3$ | • XRD<br>• SEM<br>• Weight precipitates                   | • Microwave radiation ( $\nu = 2.45 \text{ GHz}$ )<br>• Co-treatment<br>• 0.16 T<br>• Permanent magnets<br>• Co-treatment | Lab-scale<br>250 mL  | • High microwave exposure times gave in a high percentage yield of aragonite, while low exposure time favored vaterite formation.  | 104  |
| High and low supersaturated $\text{CaCO}_3$ solution  | • Concentration of Ca                                     | • 0.52 T<br>• Permanent magnets<br>• Pretreatment   | Lab-scale 1 L        | • EMF increased the total precipitates and favored the homogeneous nucleation<br>• EMF effects depended on pH, flow rate and residence time  | 45   |
| $\text{Na}_2\text{CO}_3$ and $\text{CaCl}_2$ mixing solutions in a test cuvette   | • UV-Vis  | • 0.55 T<br>• Permanent magnets<br>• Co-treatment   | Lab-scale            | • EMF strengthened ion interactions and increased precipitation in high supersaturated solution<br>• EMF weakened hydrate ion interaction in low supersaturated solution   | 133  |
| $\text{Na}_2\text{CO}_3$ and $\text{CaCl}_2$  | • Weight precipitates                                     | • 0.75 T<br>• Permanent magnets<br>• Co-treatment   | Lab-scale<br>10 mL   | • No difference for nucleation between untreated and EMF-treated solutions<br>• Faster sedimentation for $\text{CaCO}_3$ exposed to EMF  | 46   |
| 530 mg/L $\text{Na}_2\text{CO}_3$ and 560 mg/L $\text{Ca}(\text{NO}_3)_2 \cdot 4 \text{H}_2\text{O}$  | • UV350<br>• Turbidity<br>• SEM                           | • 10–100 kHz<br>• Pulsed-EMF<br>• Pretreatment  | Lab-scale<br>600 mL  | • EMF increased the generation of critical nuclei<br>• The formation of calcite promoted the dissolution of smaller crystals   | 47   |
| $\text{Ca}^{2+}$ , $\text{CO}_3^{2-}$ , and $\text{HCO}_3^-$ , 300–500 mg/L as $\text{CaCO}_3$  | • Weight precipitates<br>• XRD                            | • Permanent magnets<br>• Co-treatment   | Lab-scale<br>500 mL  | • The EMF device with more irregular waveform enhanced particulate aggregation and changed the crystal morphology  | 101  |
| $\text{CaCl}_2$ and $\text{Na}_2\text{CO}_3$ at 0.5 M.<br>$\text{CaCl}_2$ and $\text{Na}_2\text{SO}_4$ at 0.5 M.<br>$\text{BaCl}_2$ and $\text{Na}_2\text{SO}_4$ at 0.5 M.  | • Concentrations of scaling ion<br>• Turbidity            | • 0.16 T<br>• Permanent magnets<br>• Co-treatment   | Lab-scale<br>500 mL  | • EMF increased total precipitate<br>• Homogeneous nucleation was promoted by increasing pH, flow rate and residence time<br>• The presence of $\text{CaCO}_3$ colloid particles was not necessary   | 103  |
| Potable water.<br>Seawater  | • TSS<br>• Hardness<br>• Water chemical composition       | • 0.16 T<br>• Permanent magnets<br>• Co-treatment   | Lab-scale            | • EMF reduced $\text{CaCO}_3$ , $\text{CaSO}_4$ , and $\text{BaSO}_4$ scaling<br>• EMF effect on $\text{CaSO}_4$ was stronger than $\text{CaCO}_3$ and $\text{BaSO}_4$   | 49   |
| 53 g/L $\text{Na}_2\text{CO}_3$ and 56 g/L $\text{CaCl}_2$  | • Carbonate concentration                                 | • 0–0.96 T<br>• Permanent magnets<br>• Pretreatment   | Pilot-scale<br>945 L | • EMF did not change chemical composition, hardness, organic materials and trace metals of potable water, but reduced TSS<br>• Negligible changes of seawater  | 49   |
|   |   |   | Lab-scale            | • The inhibition of $\text{CaCO}_3$ scaling enhanced as increasing EMF intensity<br>• The EMF effectiveness increased as increasing temperature<br>• Maximum EMF effect at critical flow velocity<br>• pH had negligible impact<br>• Effect of velocity was larger than other parameters | 134  |
| $\text{Ca}(\text{HCO}_3)_2$ solution  | • XRD<br>• TEM<br>• EDX                                   | • 0.5 and 1.3 T<br>• Permanent magnets<br>• Co-treatment  | Lab-scale            | • Different EMF intensity changed calcite/aragonite/vaterite ratio<br>• Aragonite increased with EMF, scaling was prevented in turbulent flow  | 100  |
| Geothermal water  | • Weight precipitates<br>• $\text{Ca}^{2+}$ concentration | • Solenoid coils<br>• Pretreatment  | Lab-scale            | • EMF decreased the total deposit significantly  | 102  |



**Table 3** continued

| Solution  | Characterization  | EMF/Treatment  | Set-up    | EMF anti-scaling effect   | Ref.           |
|---|---|--|-----------|---|----------------|
| 30 mmol/L $\text{Ca}(\text{HCO}_3)_2$ solution  | <ul style="list-style-type: none"> <li>pH</li> <li><math>\text{Ca}^{2+}</math> concentration</li> <li>XRD</li> <li>SEM</li> </ul> | <ul style="list-style-type: none"> <li>Solenoid coils</li> <li>2000 Hz, 3 A</li> <li>Pretreatment</li> </ul> | Lab-scale | <ul style="list-style-type: none"> <li>EMF hindered the precipitation of <math>\text{CaCO}_3</math> and inducing <math>\text{CaCO}_3</math> precipitates as vaterite crystals</li> <li>EMF could improve the effect of scale inhibitor</li> </ul>   | <sup>135</sup> |
| 10 mmol/L $\text{Ca}(\text{HCO}_3)_2$ and $\text{Mg}(\text{HCO}_3)_2$ solution  | <ul style="list-style-type: none"> <li>pH</li> <li>Conductivity</li> <li>Turbidity</li> <li>XRD</li> <li>SEM</li> </ul>           | <ul style="list-style-type: none"> <li>Solenoid coils</li> <li>2000 Hz, 3 A</li> <li>Pretreatment</li> </ul> | Lab-scale | <ul style="list-style-type: none"> <li>EMF and ultrasonic decreased the particle size and accelerated the precipitation of <math>\text{CaCO}_3</math></li> <li><math>\text{Mg}^{2+}</math> presence made the particles larger and looser structure</li> </ul>   | <sup>136</sup> |
| pH 6.4; alkalinity 16 mg/L; TDS 38 mg/L; EC 56 $\mu\text{S}/\text{cm}$  | <ul style="list-style-type: none"> <li>pH</li> <li>Alkalinity</li> <li>Ion concentrations</li> <li>Conductivity</li> </ul>        | <ul style="list-style-type: none"> <li>0.05–0.2 T</li> <li>Pretreatment</li> </ul>                           | Lab-scale | <ul style="list-style-type: none"> <li>EMF increased the solution content of <math>\text{Mg}^{2+}</math>, <math>\text{K}^+</math>, <math>\text{Na}^+</math>, <math>\text{Cl}^-</math>, alkaline and <math>\text{SiO}_2</math>, decreased <math>\text{Ca}^{2+}</math> and <math>\text{SO}_4^{2-}</math></li> <li>pH, EC and TDS increased with increasing EMF intensity</li> </ul> | <sup>137</sup> |
| XRD X-ray diffraction, SEM scanning electron microscopy, EDX energy dispersive X-ray spectroscopy, EC electrical conductivity, UV–Vis ultraviolet-visible light, TH total hardness, TSS total suspended solids, TEM transmission electron microscopy, PSD particle size distribution, T tesla (unit). |   |  |           |   |                |

crystallization through increasing the total precipitate quantity and favoring its formation in the bulk solution instead of its incrustation on the walls. Szkatula et al.<sup>45</sup> conducted two large-scale experiments of magnetic treatment of industrial water. One of them was operated with two identical 25 kW heat exchangers for 4 months. The amount of deposit which composed mostly of calcite, reached 20 g/m of tube at the warm end of the heat exchanger, while the mass of the deposit for EMF-treated water was only 0.5 g/m of tube, which composed mainly of non-crystalline silica-rich material. Further results from the practical installation at three blocks of a 1 GW power plant implied that colloidal silica was able to adsorb calcium, magnesium or other metal ions and then precipitated from the solution as the coagulated agglomerate, as a consequence, the scaling on the walls of pipes and vessels reduced. Even though several lab-scale tests observed the enhanced precipitation of  $\text{CaCO}_3$  with the EMF treatment due to increasing nucleation or faster sedimentation, all these precipitations remained in the bulk solution instead of the reactor walls<sup>46–49</sup>.

The only ineffective case came from Salman et al.<sup>50</sup> when they investigated the effect of EMF on potable water and seawater. The results demonstrated that EMF affected clearly the turbidity and total suspended solids of tested water, but it did not change the chemical composition, hardness, organic materials and trace metals of both potable water and seawater. Although EMF had no impact on potable water and seawater in the pilot-scale testing, EMF was successful to reduce  $\text{CaCO}_3$ ,  $\text{CaSO}_4$ , and  $\text{BaSO}_4$  scaling in the small lab-scale testing with synthetic solutions<sup>50</sup>. As a consequence, the efficiency of EMF depended on different parameters such as water chemistry, flow rate, operating parameters, and magnetic power. The impact of operating conditions on EMF treatment will be discussed in section “Operating Conditions of EMF Treatment”.

#### EMF treatment on membranes

Contrary to the successful use of EMF in heat reactors, bulk solutions, and pipes, 14% studies reported EMF applications in membrane systems were not as effective. Higher percentage of ineffective cases for membrane systems results from more complex configuration and operation as compared to bulk solutions, reactors, and pipes. The operating parameters like presence of spacers and water recovery, significantly influence EMF treatment (section “RO System Operation”). Pelekani et al.<sup>51</sup> and Carnahan et al.<sup>52</sup> studied the impact of EMF on RO separation for saline groundwater and synthetic salt solutions, respectively, but no significant improvement of EMF treatment was observed.

In some other cases, the EMF treatment was reported to be effective for impeding scale formation on membrane surfaces. The positive effect of EMF was proven through the lower permeate flux decline in NF<sup>53</sup> and MD<sup>54</sup> systems or less scaling on UF<sup>55</sup> and RO membranes<sup>56</sup>. A study by Palmer et al.<sup>56</sup> used the Grahamtek electromagnetic anti-scaling technology on a large scale industrial wastewater treatment system. The wastewater had a total dissolved solids (TDS) concentration of 5,500–7,500 mg/L and contained significant amounts of ammonia, sulfate, magnesium, and silica. The EMF treatment was effective in preventing magnesium silicate scale formation at water recovery over 85%, but  $\text{BaSO}_4$  tended to form an amorphous deposit on membrane surface. On the other hand, some studies with spiral wound RO system has testified the validity of EMF treatment to eliminate membrane scaling and enhance bulk precipitation, even though these precipitates blocked concentrate flow and decreased permeate flux<sup>57,58</sup>. A Descal-A-Matic device was used to provide EMF that was expected to neutralize minerals and dissolved solids during desalination of saline drainage water<sup>57</sup>. It was observed that the water recovery decreased faster with the treatment of

**Table 4.** Summary of recent EMF water treatment studies on membranes.

| Solution   | Characterization   | EMF/Treatment  | Set-up  | EMF anti-scaling effect  | Ref. |
|--|--|--|---|--|------|
| 1,880–3,000 mg/L $\text{CaCO}_3$   | <ul style="list-style-type: none"> <li>• UTDR</li> <li>• SEM</li> <li>• XRD</li> <li>• Permeate flux</li> </ul>                          | <ul style="list-style-type: none"> <li>• 0.02 T</li> <li>• Permanent magnets</li> <li>• Pretreatment</li> </ul>  | Lab-scale NF 5 L  | <ul style="list-style-type: none"> <li>• EMF suppressed calcite and favored vaterite and aragonite.</li> <li>• EMF enhanced permeate flux by 6–10%</li> </ul>  | 52   |
| Tap water: TH 89–100 mg/L as $\text{CaCO}_3$ , alkalinity 132 mg/L as $\text{HCO}_3^-$   | <ul style="list-style-type: none"> <li>• SEM-EDX</li> <li>• XRD</li> <li>• Permeate flux</li> </ul>                                      | <ul style="list-style-type: none"> <li>• 0.1 T</li> <li>• Permanent magnets</li> <li><i>RWE-S Magnetizer Group Inc., USA</i></li> <li>• Pretreatment</li> </ul>    | Lab-scale MD  | <ul style="list-style-type: none"> <li>• EMF formed larger crystallites and more porous deposit</li> <li>• EMF improved permeate flux by 10–25%</li> </ul>   | 53   |
| Synthetic water: Kaolinite 5 mg/L, NOM 777 mg/L, NaCl 2,950 mg/L, $\text{NaHCO}_3$ 42 mg/L   | <ul style="list-style-type: none"> <li>• UV254 for NOM</li> <li>• SEM</li> <li>• FT-IR</li> <li>• Permeate flux</li> </ul>               | <ul style="list-style-type: none"> <li>• 0–2 V/cm</li> <li>• Permanent magnets</li> <li>• Co-treatment</li> </ul>  | Lab-scale UF<br>1.4 L 30 kPa  | <ul style="list-style-type: none"> <li>• Combined coagulation and EMF mitigated membrane fouling with the improvement of 33–50% water flux and 83% organic rejection</li> <li>• More porous and hydrophilic cake layers under higher EMF strengths</li> <li>• The electrolyte concentration exhibited little effect on water flux</li> </ul> | 54   |
| 550 mg/L $\text{CaCO}_3$   | <ul style="list-style-type: none"> <li>• SEM</li> <li>• Permeate flux</li> <li>• Salt rejection</li> </ul>                               | <ul style="list-style-type: none"> <li>• 25 A, 50 Hz</li> <li>• Solenoid coils</li> <li>• Co-treatment</li> </ul>  | Lab-scale RO 25 L   | <ul style="list-style-type: none"> <li>• EMF improved the 5.3% salt rejection and 30% permeate flux</li> </ul>   | 77   |
| 11 g/L of salts including Ca and Mg compounds  | <ul style="list-style-type: none"> <li>• SEM</li> <li>• EDX</li> <li>• Permeate flux</li> </ul>  | <ul style="list-style-type: none"> <li>• Pulsed-power EMF</li> <li><i>Cleanwater Systems LLC Dolphin system</i></li> <li>• Pretreatment</li> </ul>                 | Pilot-scale RO  | <ul style="list-style-type: none"> <li>• EMF eliminated most scaling</li> <li>• Precipitates blocked concentrate flow</li> </ul>   | 57   |
| 11 g/L of salts including Ca and Mg compounds  | <ul style="list-style-type: none"> <li>• Permeate flux</li> </ul>  | <ul style="list-style-type: none"> <li>• Pulsed-power EMF</li> <li><i>Cleanwater Systems LLC</i></li> <li><i>Dolphin system</i></li> <li>• Pretreatment</li> </ul> | Semi-pilot RO   | <ul style="list-style-type: none"> <li>• EMF reduced scaling on membrane, but precipitates block concentrate flow</li> <li>• Smaller crystals formed and packed more tightly</li> </ul>  | 57   |
| 1,350 mg/L TDS iron-rich, saline groundwater   | <ul style="list-style-type: none"> <li>• SEM</li> <li>• Permeate flux</li> </ul>   | <ul style="list-style-type: none"> <li>• 320 Hz</li> <li>• Solenoid coils</li> <li><i>GrahamTek Singapore</i></li> <li>• Co-treatment</li> </ul>                   | Pilot-scale RO 270 $\text{m}^3/\text{day}$ 31–33 L/ $\text{m}^2/\text{h}$ | <ul style="list-style-type: none"> <li>• Ineffective at 80% recovery; the chemical cleaning period increased from 3–4 days to 5 days</li> <li>• Effective at 70% recovery; the cleaning period increased to 18–38 days</li> </ul>  | 50   |
| Saline drainage water: $\text{Ca}^{2+}$ 68–91 mg/L, No carbonate, $\text{Mg}^{2+}$ 45–63 mg/L, $\text{SO}_4^{2-}$ 766–931 mg/L, pH 5.1–6.1, TDS 2,030–2,410 mg/L | <ul style="list-style-type: none"> <li>• Permeate flux</li> </ul>  | <ul style="list-style-type: none"> <li>• Magnetic core</li> <li>• channel</li> <li><i>Descal-A-Matic</i></li> <li>• Co-treatment</li> </ul>                        | Pilot-scale RO  | <ul style="list-style-type: none"> <li>• Ineffective; significant <math>\text{CaSO}_4</math> scaled on feed spacer with EMF</li> </ul>   | 56   |
| Raw wastewater: TDS 5000–7500 mg/L, $\text{SiO}_2$ 20–60 mg/L, $\text{SO}_4^{2-}$ 11 g/L of salts including 3500–5000 mg/L, $\text{Mg}^{2+}$ 400–700 mg/L        | <ul style="list-style-type: none"> <li>• SEM</li> <li>• Permeate flux</li> </ul>   | <ul style="list-style-type: none"> <li>• 415 V, 50–400 Hz</li> <li>• Solenoid coils</li> <li><i>GrahamTek</i></li> <li>• Co-treatment</li> </ul>                   | Pilot plant RO  | <ul style="list-style-type: none"> <li>• EMF inhibited magnesium silica scaling</li> <li>• <math>\text{BaSO}_4</math> tended to form an amorphous deposit</li> </ul>   | 55   |
| LiCl, NaCl, KCl, $\text{MgCl}_2$ , and $\text{CaCl}_2$ at 0.02 M, 0.05 M, 0.1 M  | <ul style="list-style-type: none"> <li>• Salt rejection</li> </ul>   | <ul style="list-style-type: none"> <li>• 0.068 T, 40–300 Hz</li> <li>• Solenoid coils</li> <li>• Co-treatment</li> </ul>   | Lab-scale RO 200 L  | <ul style="list-style-type: none"> <li>• No differences in the salt permeability were observed</li> </ul>  | 51   |
| Groundwater with primarily $\text{CaSO}_4$ type: TDS 5,850 mg/L; hardness 2,500 mg/L as $\text{CaCO}_3$  | <ul style="list-style-type: none"> <li>• Permeate flux</li> <li>• Salt rejection</li> <li>• XRD</li> <li>• SEM</li> <li>• EDX</li> </ul> | <ul style="list-style-type: none"> <li>• 1.2 W, 150 kHz</li> <li>• HydroFLOW Models S38 and HS48</li> <li>• Pretreatment</li> </ul>                                | Pilot-scale RO<br>22.7 L/min  | <ul style="list-style-type: none"> <li>• EMF reduced scaling and improved 38.3% and 14.3% water permeability decline rate after 150-h and 370-h operation</li> <li>• Fouling layer with EMF was loose with a low density and easily removed by hydraulic flushing</li> </ul>   | 138  |

NF nanofiltration, MD membrane distillation, UF ultrafiltration, RO reverse osmosis, UTDR ultrasonic time-domain reflectometry, XRD X-ray diffraction, SEM scanning electron microscopy, EDX energy dispersive X-ray spectroscopy, FT-IR Fourier-transform infrared spectroscopy, TH total hardness, TDS total dissolve solids, NOM natural organic matter, T tesla (unit).

EMF. Further analysis of deposit indicated significant  $\text{CaSO}_4$  scaling on the RO feed spacer, resulting in the decline of water recovery. This result provided another evidence that EMF boosts bulk precipitation of crystals rather than adhesion to membrane surface. However, the precipitates were captured and accumulated in the RO spacer mesh, clogged the feed water flow channel, caused the drop in water recovery.

## SCALING PREVENTION MECHANISMS

Several mechanisms have been proposed to explicate the various EMF effects on salt solutions. Based on the literature review, we summarize them into two fundamentally different approaches: (i) hydration effects, and (ii) magnetohydrodynamic phenomena under continuous flow condition<sup>18,42,44,46</sup>. Both mechanisms are the results of Lorentz forces—forces acting on a moving charged

particle in an EMF. Lorentz forces have been proposed to be responsible for different phenomena, including dissolution-enhancement<sup>59,60</sup>, crystallization nuclei formation<sup>61</sup>, stabilization of coordinated water<sup>62</sup>, and double layer distortion<sup>63</sup>.

#### Hydration effect

Most of the observed EMF effects can be elucidated in the light of magnetically induced changes in the hydration of ions, gas/liquid interfaces, and hydrophobic solid surfaces, which also account for the impacts observed under the static or quiescent treatment conditions (i.e., without the flow of the treated fluid phase through the EMF)<sup>18,64</sup>. It has been reported that the EMF is able to accelerate the crystallization of sparingly soluble diamagnetic salts of weak acids such as carbonates and phosphates. The mechanisms involve changing the orientation of the proton spin, thereby disturbing hydration effects by hindering the transfer of the proton to a water molecule<sup>65,66</sup>.

Stabilization of the hydration shell of scale forming ions favors dissolution because the dehydration and precipitation are more difficult to achieve<sup>67</sup>. Besides, correlation in dissolution rates with the ionic surface tension increment has been also reported<sup>68</sup>. Hence, the hydration effect is positively associated with surface tension of water that determines the interfacial interactions between water molecules and scale forming ions or solid surfaces. Some researchers noticed variations in the surface tension of water with the presence of EMF, while others discovered negligible impact. Cho and Lee<sup>69</sup> used both permanent magnet and solenoid coil device to investigate whether EMF treatment can change the surface tension of a hard water. They found that as the EMF exposure time increased, the surface tension of the tested water decreased. Besides, Pang et al.<sup>70,71</sup> also found EMF depressed surface tension force of water. This observation agreed with the result of the dye flow-visualization experiment<sup>70,71</sup>. Surface tension can be defined as the surface energy per unit area, and in the aqueous system, the surface energy of a solid–liquid state is more than that of a liquid–liquid state<sup>72,73</sup>. The presence of colloidal particles increases the surface energy at the water–colloid interface, thereby declining the surface energy at the water–reactor surface. It was also suggested that the results can be used to qualitatively evaluate the efficiency of EMF for the prevention of scaling in heat exchangers<sup>69</sup>. In contrast, some researchers reported an increase<sup>74,75</sup> or no alternation in surface tension<sup>76</sup>.

#### Magnetohydrodynamic phenomena

Magnetohydrodynamic phenomena exist only when both the treated fluid flows and the EMF presents<sup>62,77</sup>, such as in dynamic treatment conditions. The proposed magnetohydrodynamic mechanisms consider all observed effects of the dynamic EMF treatment because of the action of the Lorentz force—a force that acts on charged species when they pass through the EMF. The magnitude of this force is defined by the following equation<sup>18</sup>:

$$|F_L| = q|v \times B| = qvB \sin \theta, \quad (1)$$

where  $q$  is the quantity of charge,  $v$  is its velocity,  $B$  is the magnetic induction, and  $\theta$  is the angle between  $v$  and  $B$  vectors. Since this force can stimulate all charged species in the electrolyte solution/dispersion traversing the EMF, including the surface charge, ions in the electrical double layer near charged surfaces, and free ions in the solution. The magnetohydrodynamic mechanisms can be used to explain a wide variety of EMF effects, such as the effect of fluid velocity, magnetic induction on the quantity and crystal structure of the scale, and the main scale component (as discussed in section “Properties of EMF, Pipe Materials & Fluid Flow Rate/Velocity”).

#### Other mechanisms

Depending on the affected objects, the proposed EMF mechanisms can also be broadly categorized under (even though the nature of mechanisms is identical)<sup>8</sup>: (i) intra-atomic effects, such as changes in electron configuration as discussed in hydration effects; (ii) contamination effects caused by magnetically enhanced dissolution, like the impurities dissolved from devices or pipes; (iii) inter-molecular/ionic effects, e.g., the hydration of ions alters by EMF; (iv) interfacial effects, including alteration of gas/liquid interfaces, and hydrophobic solid surfaces.

#### CHARACTERIZATION OF EMF EFFECTS

The characterization methods to monitor the precipitation and growth of a scale layer is of great importance to quantify EMF treatment efficiency. As discussed in section “Summary of Recent EMF Treatment Studies”, the results of previous studies are somewhat contradictory because the mechanisms of EMF on scale formation and growth remain obscure, probably due to limited analytical methods and lack of quantitative studies. Hence, in the present work, we reviewed conventional characterization methods, current and potential real-time monitoring approaches for evaluation of EMF effects.

##### Conventional characterization methods

As shown in Tables 1–4, most of the EMF scaling prevention studies have provided the precipitation data as an indicator of EMF efficiency. The total precipitation is usually calculated by the change of ionic calcium concentration or solution conductivity. The bulk/homogeneous precipitation is the weight of precipitates recovered by filtration. The heterogeneous precipitation, which is adherent to the reactor surface, is determined by subtracting bulk/homogeneous precipitation from total precipitation. X-ray diffraction (XRD), scanning electron microscopy (SEM), transmission electron microscopy (TEM), and energy dispersive X-ray spectroscopy (EDX) have been used to analyze the crystal structure, morphology, and element composition of the precipitates. Although these data are very helpful to characterize scaling, there is a need for more scientific evidence on the scaling prevention mechanisms. A comprehensive understanding of scaling at the atomic level and the development of real-time monitoring for early detection of scale formation are vital for EMF applications.

##### Current real-time monitoring methods

For membrane systems, such as reverse osmosis (RO)<sup>51,56,57,78</sup>, nanofiltration (NF)<sup>53</sup>, ultrafiltration (UF)<sup>55</sup>, and membrane distillation (MD)<sup>54</sup>, water/permeate flux and salt rejection have been widely used at both lab-scale and pilot-scale to assess the EMF effectiveness on scaling control. The limitation associated with salt rejection is that it usually does not show differences with or without EMF treatment. It is challenging to distinguish the reasons for water flux decline between adherent membrane scaling and bulk precipitation. The bulk precipitation is difficult to measure because most precipitates are retained in the membrane systems.

Gabrielli et al.<sup>1</sup> built a customized magnetic device with permanent magnets to treat scaling waters and plotted chronoamperometric curves and chrono-electrogravimetric curves to estimate the scaling time and the nucleation time of the scale deposition. The two electrochemical curves were recorded by a potentiostat with the oxygen reduction current and the deposited mass as a function of time. In chronoamperometric curves, the decrease of the current flowing through the electrode demonstrated the growth of the scale on the electrode. Here, a scaling time was defined when the current reached very close to the residual current where the electrode was totally scaled. The mass deviation in chrono-electrogravimetric curves implied the mass of



scale deposited on the electrode surface, and the nucleation time was determined as the mass neatly increased after some delay. The scaling time and the nucleation time were higher in the presence of EMF and increased as increasing number of magnets. They believed that the EMF trapped a part of the ionic calcium and deactivated them from scaling. The trapping effect may be related to the surface tension of water after EMF treatment. Surface tension of the solution can be measured by tensiometer or customized capillary-tube system<sup>69,76</sup>. However, as discussed in section "Hydration Effect", the results of the surface tension are controversial. There could be a number of reasons for the different consequences, including solution impurities, temperature, and treatment time.

Natural suspended particle fragmentation with the installation of EMF device was investigated by Stuyven et al.<sup>45,79</sup>. They studied the size distribution of natural suspended particles through dynamic light scattering and applied this approach to evaluate the effect of magnetohydrodynamic forces (refer to section "Magnetohydrodynamic Phenomena") on the natural particles in tap water. They noted that natural suspended particles are disrupted into nanoscopic fragments when passing through an EMF. The size of suspended salt particles was reduced by two to three orders of magnitude indicating an increase of suspended particulate surface area by four to six orders. Under the conditions of supersaturation (e.g., heating), precipitation arises to a great extent on the large surface area of nanoparticles in the bulk solution, instead of on the limited surface area of a container or heating elements. This finding explains higher precipitation in bulk solution for most EMF studies as discussed in section "Summary of Recent EMF Treatment Studies". Similarly, Kney and Parsons<sup>47</sup> used UV-Vis spectrophotometer to measure the absorbance of the tested solution. Peak absorbance appeared when the maximum number and size of particles was reached, after that a decrease was observed owing to sedimentation and/or crystallization. They noticed when a small volume of a magnetically conditioned  $\text{CaCO}_3$  precipitate was added to a freshly mixed  $\text{Na}_2\text{CO}_3$  and  $\text{CaCl}_2$  solution, a secondary precipitate formed and settled at an accelerated rate as compared to tests using non-magnetically treated  $\text{CaCO}_3$  seed. However, they were unable to confirm the specific mechanism that led to the changes.

Although electrochemical tests (chronoamperometric and chrono-electrogravimetric curves), surface tension measurement, and optical instrument analysis can provide important information on the changes of water, particles, and precipitation with or without EMF treatment, they are all limited to small laboratory scale. Ultrasonic time-domain reflectometry is an in situ, non-invasive real-time technique that has the potential in larger scale testing. This technique has been successfully applied to analyze membrane compaction, fouling and cleaning<sup>80–85</sup>. The increase and the movement of differential signal as function of reaction time are associated with the deposition of the  $\text{CaCO}_3$  scale layer and an increase in the thickness of the fouling layer. Mairal et al.<sup>83</sup> employed the ultrasonic technique as a real-time characterization of RO membrane scaling. Pellegrino et al.<sup>58</sup> used acoustic spectroscopy to measure the ultrasonic signal attenuation coefficient as a function of frequency or ultrasonic travel velocity in the solutions. Li et al.<sup>53</sup> used this technique for quantitative study of crossflow nanofiltration to study the effect of EMF on  $\text{CaCO}_3$  scale deposition on the membrane surface. The ultrasonic testing suggested that EMF treatment could suppress and delay the initiation and precipitation of  $\text{CaCO}_3$  crystals on the membrane surface, consistent with the research results by Gabrielli et al.<sup>1</sup>.

#### Potential real-time monitoring methods

Some other real-time monitoring methods associated with microscope may be suitable for EMF anti-scale experiment. Chen

et al.<sup>86</sup> and Antony et al.<sup>9</sup> have reviewed the direct observation of foulant accumulation on the membrane surface and fouling layer formation. All the techniques studied were applied to low pressure membrane operations. For plate and frame membrane cells such as RO<sup>87</sup> and MD systems<sup>88</sup>, direct visual observation and real-time monitoring of mineral surface scaling were developed. Images of membrane surface were obtained by high resolution digital photography using an optical microscope with lighting arrangement, aiming to enhance the boundaries of semi-transparent crystals and to provide the most straightforward visualization of membrane fouling. Then the nucleation and growth of scale were quantified in a plate and frame membrane cells, detected by real-time analysis of the recorded images and the evolution of the surface number density, size of mineral crystals and the percent of surface area covered by scale<sup>87,89,90</sup>. This technique has also been applied in full scale plants to detect the scale formation by connecting this detector to a side-stream from the tail element of a spiral wound RO module, quantified by the observed crystallization induction time or the threshold surface scale coverage<sup>87,90</sup>.

Furthermore, during the fabrication of colloidal arrays, Gong and Wu<sup>91</sup> observed the movement of colloidal particles through a charge-coupled device camera that was connected to an inverted microscope. When an EMF was applied, each particle acquired an induced dipole moment and started to move. This technique provides another way to observe the movement of the particles under the exposure of EMF at atomic level.

Apart from the above methods, electrochemical impedance spectroscopy (EIS) has also been applied to various fouling and scaling related problems<sup>92–94</sup>. Comparing to current indicators for membrane fouling (e.g., pressure and water flux), EIS as a real-time monitoring approach can provide early indications of incipient fouling and scaling during separation processes<sup>92,94–96</sup>. Even though there is no research involving EIS into EMF investigation, EIS is possible to be an efficient method to monitor EMF water systems if the impact of EMF can be eliminated during EIS measurement.

## OPERATING CONDITIONS OF EMF TREATMENT

### EMF device configurations

Generally, there are two configurations of an EMF device used in water systems: permanent magnet and solenoid coil (Fig. 2). Permanent magnets have been prepared from ferromagnets of iron-based, nickel-based, cobalt-based or rare earth element-based compounds<sup>40</sup>. The EMF generated by permanent magnets depends on the arrangement and the number of permanent magnets. Some are arranged with alternating poles of magnets, others are arranged without alternations. A solenoid of electrical conducting wires can generate magnetic field within their cavity on passage of electric current<sup>97,98</sup>. The space of solenoid for linear, annular and different shape designs have been developed depending on the application<sup>40</sup>. The field strength varies with the number of coils or the thickness of the wire used. These

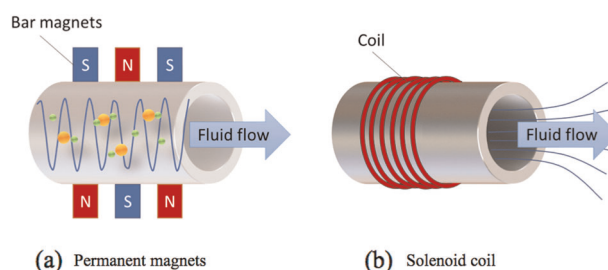


**Fig. 2 Typical EMF devices with different configurations. a Permanent magnets; b Solenoid coil.**

devices can be customized or are commercially available. Currently, most manufacturers of commercial EMF units are in the United State, Canada, Mexico, and the United Kingdom<sup>99</sup>. Besides, the generated EMF could be static or pulsating, orthogonal or parallel to the fluid flow.

EMF devices of permanent magnet and solenoid coil configurations were tested extensively in the last two decades (Tables 1–4). The efficiency of these devices remains a controversial question because of the contrastive results. On the one hand, plate-frame NF<sup>53</sup>, UF<sup>55</sup>, and MD<sup>54</sup> were investigated with the treatment of permanent magnets, the results of lab-scale tests suggested magnetic pretreatment formed more porous precipitates on the membranes. It has been also reported that CaCO<sub>3</sub> crystallization on a pipe wall declined through permanent magnets treatment<sup>44</sup>. Whereas increasing precipitation of CaCO<sub>3</sub> in bulk solution during several lab-scale tests with permanent magnets EMF treatment were reported<sup>46–48</sup>.

On the other hand, many researchers applied EMF on spiral wound RO units in treating saline wastewater or synthetic hard solution. After EMF treatment with solenoid coil configuration, Rouina et al.<sup>78</sup> found enhanced salt rejection and permeate flux, while more deposition of BaSO<sub>4</sub> was observed by Palmer et al.<sup>56</sup>. Some researchers stated limited improvement in permeate water flux<sup>51</sup> and no difference in salt permeability<sup>52</sup>. The pre-exposure of solenoid coil EMF on feed water altered the precipitation of CaCO<sub>3</sub> from forming surface nucleating scale to non-adherent bulk solution powder<sup>43</sup>. Additionally, a 20- $\mu$ m filter in the concentric tube of the heat exchanger could maintain zero fouling resistance over 820 h<sup>43</sup>. The controversial results are probably related to RO system operating conditions, such as water recovery and the presence of spacers, which will be discussed in section “RO System Operation”. Hence, EMF device configuration is not a primary factor for EMF efficiency.

#### Properties of EMF (intensity, waveform, and frequency)

The efficiency of EMF also depends on the properties of the field, including intensity, waveform, and frequency. Tai et al. used permanent magnets with different intensities [0.1 and 0.3 tesla (T)] to examine the impact of EMF on the crystal growth of calcite suspended in a fluidized bed<sup>100</sup>. The results demonstrated that the calcite growth rates in the presence of EMF were lower than those without EMF, and higher intensity yielded a reduced growth rate. Sun et al.<sup>55</sup> developed an electrocoagulation membrane reactor to treat the feed water containing clays (kaolinite) and natural organic matter (humic acid). In the electrocoagulation system, UF modules were placed between electrodes to improve effluent water quality and reduced membrane fouling. They noted that the combined effect of electrocoagulation and EMF mitigated membrane fouling in the designed reactor, resulting in higher water flux. Magnetohydrodynamic effects induced by the EMF likely played an important role in controlling membrane fouling, especially during the process of cake layer formation. The applied current density and voltage on the electrodes controlled the formation of a scale cake layer. Higher electric field strength resulted in higher porosity and hydrophilicity of the formed cake layers. Kobe et al.<sup>101</sup> also investigated the influence of the magnetic induction on the CaCO<sub>3</sub> crystallization. Calcite was the major crystalline phase (90%) for CaCO<sub>3</sub> without EMF treatment, the percentage reduced to 80 and 29% when magnetic induction was 0.4 T and 1.2 T, respectively. Meanwhile, aragonite gradually became the major phase with increasing magnetic induction. A promising result was obtained from a pilot testing that applied EMF to tap water in heat exchangers. The authors stated that the EMF treatment can reduce the need for chemically treated tap water. Besides, when the influence of an EMF intensity was between 0.5 T and 1.3 T, the nucleation and subsequent growth of

aragonite could be successfully used as a way of preventing scale<sup>17</sup>.

Two commercial EMF devices with comparable frequencies of ~100 kHz but quite different waveforms have been used to study the scale of CaCO<sub>3</sub> under the influence of the pulsed EMFs<sup>102</sup>. Piyadasa et al.<sup>102</sup> noticed that exposure to the EMF from the device with less homogeneous waveform (Fig. 3a) can improve the quantity of CaCO<sub>3</sub> microcrystals. Gabrielli et al.<sup>1</sup> built a customized EMF device with permanent magnets to treat scaling waters, and utilized an ion selective electrode to measure the remaining ionic calcium. The permanent magnets of the EMF device had two configurations: inverted and non-inverted, and the corresponding waveforms are presented in Fig. 3b. The inverted configuration had a less homogeneous waveform than non-inverted one, resulting in the nucleation delay for 5–12 times. Stojiljkovic et al.<sup>103</sup> examined the effect of different EMF waveforms generated with a home-made device on deposit formation in installations with a geothermal water. By applying the saw-tooth and sinusoidal function, the total amount of deposit in the pipe decreased from 2.07 grams (g) without EMF to 0.23 g and 0.30 g, respectively.

Yet, Carnahan et al.<sup>52</sup> investigated the effects of EMF frequency on salt and water transport in commercial and lab-scale RO membranes. During more than 500-h operation, no differences in salt permeability were observed when the frequency of EMF was varied from 40 to 300 Hz.

#### Placement of EMF devices

The placement of EMF devices in a water system might also be an important factor for the scale control efficiency. Most previous studies using EMF exposure as a pretreatment for feed water acquired positive results, including the experiments on heat exchangers<sup>17,42,43,79</sup>, membranes<sup>53,54</sup>, pipes<sup>1</sup>, as well as bulk solutions<sup>18,79,102</sup>. The quantity of scale precipitated in boilers and pipes in heat exchangers after three-weeks operation was measured to evaluate the EMF efficiency<sup>42</sup>. Tap water was exposed to EMF before entering the boilers, scales occurred in much smaller amounts: the scale on heating copper-pipe spiral was 2.5 times thinner and only very thin powder-like coating was observed in zinc-coated steel pipe, while abundant hard lining was formed in absence of EMF. The crystals on boilers were about four times thinner in the case of EMF. Stuyven et al.<sup>45</sup> used EMF to pretreat potable water and found disaggregation of suspended particles in turbulent flow. Other studies observed larger quantity of precipitates in the bulk solution with pre-exposure to EMF instead of reactor walls<sup>102,104</sup>.

The influence on efficiency is more polytropic when an EMF device is placed directly on the scaling surface (referred as co-treatment in Tables 1–4). Salman et al.<sup>50</sup> reported no change of chemical composition of both potable water and seawater in the water tank. As for the research conducted on spiral wound RO units, Rouina et al.<sup>78</sup> found improvement of both salt rejection and permeate flow rate, while Pelekani et al.<sup>51</sup> reported limited enhancement of permeate flux. Others presented more precipitations of CaSO<sub>4</sub><sup>57</sup> and BaSO<sub>4</sub><sup>56</sup> on the membrane or spacer surface, while there was no difference in salt permeability<sup>52</sup>. The variation might be derived from the impact of water recovery, feed water composition, and the presence of spacer in RO system (as discussed in section “RO System Operation & Water Chemistry”).

#### Exposure time to EMF

EMF exposure time affects both quantity and morphology of precipitation. Alimi et al.<sup>46</sup> investigated the influence of the EMF exposure time on the precipitation in the tested solution. They found an optimal treatment time of approximately 15 min that corresponded to higher total precipitation and bulk precipitation of CaCO<sub>3</sub> at different fluid flow rates. The authors claimed that the

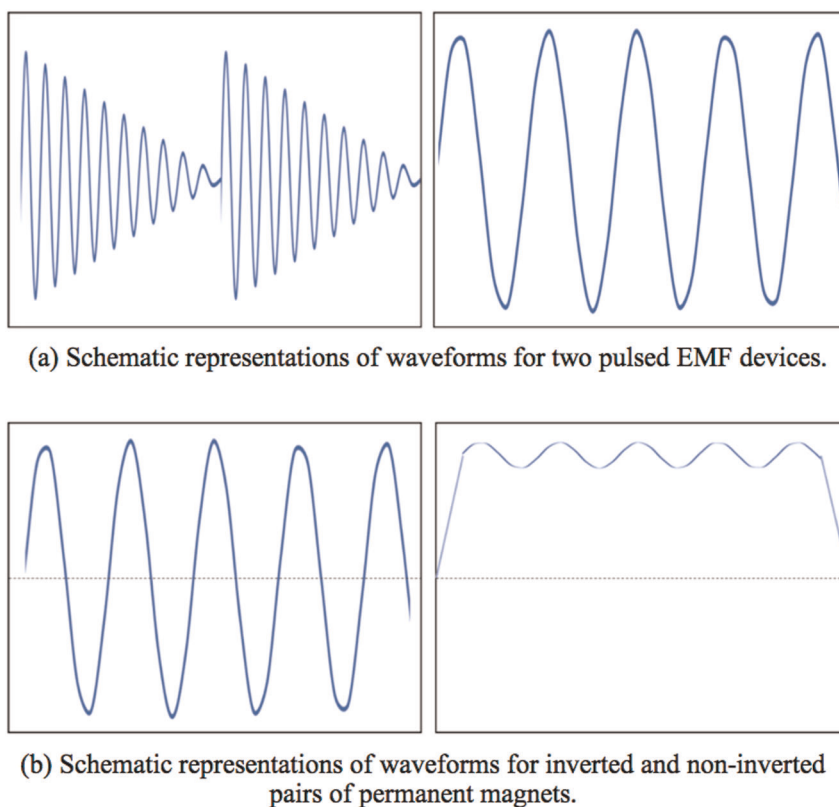


**Fig. 3** Waveforms of EMF discussed in the present work. **a** Schematic representations of waveforms for two pulsed EMF devices; **b** Schematic representations of waveforms for inverted and non-inverted pairs of permanent magnets.

induction time for  $\text{CaCO}_3$  nucleation was remarkably declined with the exposure of EMF, so the micellization of ionic pairs was more advanced, and then accelerated the effective nucleation process. The changes of  $\text{CaCO}_3$  precipitate quantity for different exposure time might attribute to magnetohydrodynamic phenomena.

Among different phases of  $\text{CaCO}_3$  such as calcite, aragonite, and vaterite, aragonite is considered to be a less stable phase that is thought to form less tenacious layers and can be easily washed off a substrate by fluid flow<sup>7</sup>. Knez and Pohar<sup>18</sup> performed precipitation tests to determine the influence of EMF exposure time on synthesized calcium hydrogen carbonate solution. EMF favored the precipitation of aragonite and the aragonite content increased with increasing exposure time to EMF. In addition, tests conducted by Rizzuti et al.<sup>105</sup> claimed that EMF treatment preferred the precipitation of aragonite with increasing exposure time, while vaterite formation of  $\text{CaCO}_3$  was supported by low exposure time. Similar result was reported by Tai et al.<sup>100</sup> that the yield of crystalline phases depended on the EMF exposure time, where aragonite was predominant phase with longer exposure time. Besides, some researchers confirmed that the memory effect of EMF can last up to 200 h after the EMF removed<sup>19</sup>.

#### RO system operation

As discussed in section “EMF Device Configurations”, the EMF performance on RO systems is polytropic, largely coming from the system operational conditions. At water recovery higher than 80%, EMF treatment can reduce scaling on membrane surface, but the bulk precipitates scaled on feed spacer or blocked concentrate flow, as a consequence of permeate flux decline<sup>51,57,58</sup>. Whereas, Pelekani et al.<sup>51</sup> reported 8 times improvement on chemical cleaning required period compared to non-EMF treatment when the water recovery decreased to 70%, probably because less and smaller bulk precipitates were generated and easier to be washed

out. But no differences in the salt permeability were observed at water recovery of 9.3%<sup>52</sup>. Therefore, moderate water recovery is of great importance for successful EMF application in RO system. Moreover, the presence of spacer may reduce the scale suspended time significantly in the flow channel, resulting in precipitation on the spacers.

#### Pipe materials

The materials of the pipe where the EMF is applied can impact the formation of scale. The influence of pipe materials was studied by Gabrielli et al.<sup>1</sup>. Along with stainless steel, various conducting and insulating materials were tested such as copper and two types of polyvinyl chloride (PVC) referred as PVC I and PVC II. PVC I was pure PVC, and PVC II was the common tubing used in plumbing, loaded with alumina and  $\text{CaCO}_3$ . Compared with PVC I as a reference, the total precipitation increased by 18% for PVC II and 28% for stainless steel and copper. However, the authors did not provide the comparative data without EMF treatment for these pipes as references. According to the results from Alimi et al.<sup>44</sup>, the influence of the pipe materials in the absence of EMF cannot be ignored. The precipitation amount followed the order of Tygon > stainless steel > copper > polytetrafluoroethylene (PTFE), with or without EMF treatment. The application of the EMF enlarged the total and homogeneous precipitation for all used pipe materials. Although the EMF effect on precipitation is less important for copper and stainless steel, the total precipitations are still higher than EMF-treated PTFE. This observation agreed to a certain extent with the research of Gabrielli et al.<sup>1</sup>. Moreover, two pipes made of Teflon, were also tested by Alimi et al.<sup>44</sup>; a non-conductive PTFE and an electroconductive anti-static PTFE. They found that non-conductive PTFE has more improvement for calcium precipitation than electroconductive one, in contrast to Gabrielli et al.’s result<sup>1</sup>.



However, due to lack of detail information of these polymeric pipe materials, further comparison of the two papers is restricted.

Some researchers believed that the effect of the pipe materials on the total precipitation might be accompanied with the presence of impurities in the solution when passing through the tubing. It was found that leachate concentrations were the highest for Tygon, and PTFE did not leach any detectable contaminants after comparing the leachates from a variety of pipes<sup>106,107</sup>. In fact, these leachates can work as seeds that promote the precipitation in the bulk solution. Hence, the observation of Alimi et al.<sup>44</sup> became reasonable with regards to the lower precipitation perceived for PTFE and the higher homogeneous precipitation for Tygon.

Because the pipe materials have an important effect on  $\text{CaCO}_3$  precipitation, the surface state of the pipe may also influence the hydrodynamic parameters. PVC pipes with three different roughness levels were tested: smooth pipe, polished pipes using abrasive papers of 320 and 80 (roughness 320 is smoother than roughness 80). It was demonstrated that the quantities of the total and the homogeneous precipitates increased simultaneously with roughness, with or without EMF treatment<sup>44</sup>. Only the homogeneous precipitation was influenced by wall roughness. Actually, internal roughness can generate turbulence areas in the vicinity of the walls, thereby create local eddy currents<sup>108,109</sup>. Then the release of impurities by erosion is accentuated and the precipitation of  $\text{CaCO}_3$  tends to occur in the bulk solution instead of the reactor walls. The impact of roughness can be used to explain the failure cases of EMF treatment on RO system<sup>56,57</sup>, the spacers in the RO unit extend the roughness of the system, resulting in increasing scale precipitation.

#### Fluid flow rate/velocity

The effect of EMF on scaling in a double-pipe heat exchanger was investigated by Shahryari and Pakshir<sup>110</sup>. A double-loop-configuration consisting of cooling and heating water cycles was used to study the impact of cooling water flow rate on the EMF treatment efficiency. In the absence of EMF treatment, the scale deposited on the heat exchanger surface decreased with increasing cooling water flow rate. The application of EMF decreased the fouling resistance (representing heat transfer) in the heat exchanger by 76.3% compared to the untreated test, at 0.5 m/s flow rate. However, increasing the water flow rate resulted in a decrease in the EMF efficiency, where 64.3% and 57.8% drop in fouling resistance of heat exchanger at 0.8 and 1.3 m/s water flow rate, respectively. Some researchers examined the impact of flow rate on total precipitation and homogeneous precipitation of  $\text{CaCO}_3$  with different pipe materials<sup>44,46,104</sup>. Interestingly, the total precipitation was flow rate-dependent only for conductive pipes (copper and stainless steel) with the presence of EMF, whereas homogeneous precipitation was flow rate-dependent in all circumstances (flow rate: 0.23–0.41 m/s). The deposit on the surface of all pipe materials reduced at higher flow rate in absence of EMF because these precipitates were washed out by water flow. While applying EMF, the surface scale weakened for non-conductive pipes (PTFE and Tygon) with increasing flow rate but was flow rate-independent for conductive pipes. According to Eq. (1), magnetohydrodynamic phenomena depend on the flow of the treated solution. Internal roughness generates turbulence areas in the vicinity of the walls then creates local eddy currents. As a consequence, a larger velocity gradient was generated, and the balance of calcium-carbonate equilibrium was disturbed along the walls. The aggregation of the  $\text{CaCO}_3$  colloidal particles under the magnetohydrodynamic phenomena would lead to expediting the precipitation process.

Garbrielli et al.<sup>1</sup> observed an enhanced  $\text{CaCO}_3$  precipitation with increasing flow rate in a wider range. Under exposure to EMF, comparing with initial ionic calcium concentration, a

0.074 m/s velocity induced a 15% decrease of the concentration and reached 25% at a 1.8 m/s. The efficiency did not practically rise for a twice-faster velocity (3.6 m/s). Hence, the EMF efficiency is not always positively correlated to flow rate, there is a maximum efficiency at an optimal water flow for EMF treatment.

Kobe et al.<sup>101</sup> found that the flow conditions played a significant role besides the EMF to modify the crystallization phase of  $\text{CaCO}_3$ . The formation of crystals depends on the initial conditions of crystallization, which on its turn depends on the free energy of the molecular system. Moreover, if the energy density of 25 eV per molecular volume could be provided to the molecular system, then accumulation of additional  $\text{Ca}^{2+}$  and  $\text{CO}_3^{2-}$  around the initial seed, will have higher probability to give structural forms crystallized with hexagonal symmetry (aragonite). Yet, generally used EMF (0–2 T) cannot provide enough energy to bridge the gap between the ions of  $\text{Ca}^{2+}$  and  $\text{CO}_3^{2-}$ , but the presence of turbulent flow can amplify EMF effect to provide enough free energy<sup>111</sup>.

#### Water chemistry

Water chemistry of the flow solution is a critical parameter affecting scaling. Obviously, the precipitation mainly depended on the major ions of the test solution, other factors like pH, temperature, presence of particles and dissolved gas, can also influence the precipitation-dissolution equilibrium in the aquatic system.

**Major anions.** As stated in the Introduction, the formation of scale depended on the major ions of the feed water. Carnahan et al.<sup>52</sup> investigated the effects of EMF on salt and water transport in RO membranes. For both commercial RO unit and classic lab-scale RO system, no effects of the EMF were observed on the pure water permeability regarding the synthetic feed solution ( $\text{LiCl}$ ,  $\text{NaCl}$ ,  $\text{KCl}$ ,  $\text{MgCl}_2$ , and  $\text{CaCl}_2$ ).  $\text{CaCO}_3$  is the most common scale because calcium and bicarbonate are abundant in the water bodies. Thus, the majority of EMF studies have focused on  $\text{CaCO}_3$  precipitation, and based on our literature review (Tables 1–4), most of them observed a reduction of adherent scale on the surface of heat exchangers, pipes, and membrane systems in the presence of EMF. However, promoted scaling was found when the primary precipitation was sulfate-based particles, such as  $\text{CaSO}_4$ <sup>57,58</sup> and  $\text{BaSO}_4$ <sup>56</sup>.  $\text{CaSO}_4$  and  $\text{BaSO}_4$  are much tighter and smaller particles than  $\text{CaCO}_3$ , as a result, they are more difficult to be removed by water flush then packed more tightly on the membrane surface or feed spacer, finally increasing membrane resistance<sup>56–58</sup>. Different results were observed by Salman et al.<sup>50</sup> when compared the EMF effects on  $\text{CaCO}_3$ ,  $\text{CaSO}_4$  and  $\text{BaSO}_4$  scaling in bulk solution. The study confirmed that EMF was effective to reduce or retard the scale, the effect on  $\text{BaSO}_4$  was found to be stronger than on  $\text{CaCO}_3$  or  $\text{CaSO}_4$ . EMF succeeded in keeping the scale suspended for 45 min for  $\text{BaSO}_4$ , and 20 min for  $\text{CaCO}_3$ , while EMF inhibited the  $\text{CaSO}_4$  from precipitation for 10 min. Hence, the effect of EMF was proven to be selective depending on the type of scale. Since the time required for the feed water to enter and exit a desalination plant is typically less than 15 min, flow rate is also a key factor for EMF effectiveness. The different results of bulk solution and RO tests probably attribute to the presence of spacer, which may remarkably decrease the scale suspended time in RO system. A recent study on EMF application in the RO system in treating  $\text{CaSO}_4$ -riched groundwater demonstrated that EMF could reduce scaling and improved permeate flux. The EMF induced a high frequency electric signal, which could loosen colloidal particles, fouling and scaling layer on cartridge filter, membranes, and pipelines, but the shed fine solids accumulated and clogged the traditional mesh spacers in the RO feed flow channel<sup>112</sup>.

**Suspended particles.** Given that water may contain suspended particles (mainly silica and alumina), Stuyven et al.<sup>45</sup> examined the fate of waterborne natural particles passing through an EMF device. After magnetic conditioning, the water contained crystallization nuclei to promote formation of waterborne  $\text{CaCO}_3$  crystals instead of scale deposits on the surfaces of heater elements. They concluded the presence of suspended particles was a condition for EMF water treatment to be effective. In addition, Stuyven et al.<sup>79</sup> found combining hydrodynamic forces of turbulent flow with Lorentz forces generated by EMF was an energy-efficient approach to disaggregate suspended particles. As a result, more surface area of the suspended particles was provided for scale formation. Szkatula et al.<sup>113</sup> conducted two large-scale experiments of EMF on industrial water, aimed to study changes in the formation of deposits. They noted an amorphous, soft deposit recovered with EMF that came from silica hydrosol. The crystallization of carbonates in water was blocked due to the activation of the colloidal silica, which would adsorb calcium, magnesium or other metal ions. These metals and carbonates ions then precipitated from the solution as the coagulated agglomerate. The activation of silica probably came from Lorentz-force induced deformation of the diffusion layer leading to the increased counterion concentration in the adsorption layer of the negatively charged silica. Hence, the authors suggested that it was necessary to activate only a small fraction of silica present in water to prevent the system against lime scale. Furthermore, this idea could be used to explain the unsuccessful cases of EMF on RO units<sup>56,57</sup>, the spacers in the RO unit extend the surface area of the system, leading to boosted scale precipitation.

**pH.** pH has a significant effect on the results of the tests, even slight changes in pH generated different precipitation conditions. The effect of pH on precipitation is easily understandable: when the water becomes more alkaline, the calcocarbonic equilibrium is displaced towards a stronger supersaturation, then the nucleation probably gets larger<sup>104</sup>. However, the impact of pH on EMF performance is not clear. Typically, the pH throughout a testing period varies from  $\pm 0.25$  to 0.5 unit<sup>18,47</sup>. Kney and Parsons<sup>47</sup> found that by adding small volumes (i.e., 0–50  $\mu\text{L}$ ) of 0.5% NaOH to a test cuvette the variations in pH could be controlled, so that the point of accelerated precipitation could be maintained from test to test. Besides, a good repeatability of the accelerated settling conditions was achieved by adding a specific volume of NaOH (i.e., in this case 25  $\mu\text{L}$ ). It was important to note that the accelerated conditions could not be achieved if less than 25  $\mu\text{L}$  of base was added. Thus, the point of accelerated precipitation is very pH specific. Faith et al.<sup>104</sup> investigated the impact of EMF on  $\text{CaCO}_3$  crystallization at the pH range of 6–6.5. The experimental results proved that the EMF promoted preferentially the homogeneous precipitation detrimentally to the scaling of the walls, and this effect was more remarkable at lower pH. For instance, in the absence of EMF, the total precipitation ratio was 73%, of which 22.2% for the homogeneous precipitation and 50.8% for the heterogeneous precipitation. In the presence of EMF, the total precipitation ratio increased to 84%. The homogeneous contribution increased to 38.9% whereas the heterogeneous one decreased to 45.1%. Similar result was obtained by EMF-treated PTFE pipe, but simultaneous augmentation for both total and homogeneous precipitations was observed using Tygon pipe<sup>44</sup>. Overall, increasing pH accelerates precipitation in bulk solution.

**Temperature.** In neutral aquatic systems,  $\text{CaCO}_3$  exists in the form of calcium and bicarbonate ions. Dissolved calcium and bicarbonate ions do not precipitate at relatively low or moderate temperature because both ions are surrounded by water molecules<sup>43</sup>. As increasing solution temperature, the calcium ion precipitates because its solubility declines with higher temperature of solution. The scale forms preferentially on hot surfaces as

the diffusion of calcium ions is accelerated by the relatively higher temperatures around the heat exchanger surface. It has been reported that EMF can increase the solution temperature to some degree, but it is not enough to cause this intra-molecular disruption<sup>43</sup>. Nevertheless, the interactions of EMF with temperature on scaling are unclear.

In a recent review, Alabi et al.<sup>7</sup> analyzed temperature impact through three studies during 1996–1998. It was found that there was negligible difference with and without EMF treatment in the temperature range of 40–60 °C<sup>114</sup>. Higashitani et al.<sup>115,116</sup> however observed thermal dependence of EMF treatment on electrolyte and colloidal solutions. The EMF did enhance precipitation when temperature below 30 °C, but the magnetic effect waned as the temperature increased and almost disappeared at 50 °C.

Different phenomenon was detected by Lipus and Dobersek<sup>42</sup> when compared scales from two parallel experimental lines with boilers, one supplied by untreated tap water and another by the water circulated through the EMF device. They claimed that EMF reduced the thickness of scale on high-temperature (70 °C) heating surfaces and protected the hot water conducting pipes from scale completely and even dissolve old scales in the pipes. Rizzuti et al.<sup>105</sup> investigated the effect of EMF that generated inside a multimode microwave applicator on the crystallization of  $\text{CaCO}_3$  polymorphs. An increasing formation of more porous aragonite and a decreasing vaterite content were observed at higher temperature (80–90 °C). Deposition of precipitated  $\text{CaCO}_3$  from  $\text{Na}_2\text{CO}_3$  and  $\text{CaCl}_2$  solutions on different substrates, including stainless steel, copper, aluminum, and glass, was investigated at temperatures of 20 °C, 40 °C, 60 °C and 80 °C. It was found that during 2-h quiescent conditions, the amounts deposited firmly on the surfaces decreased with increasing temperature. The deposition was reduced at all temperatures with the presence of EMF, but the deposit amounts depended on the nature of the substrate. The largest EMF effect was found on glass at 60 °C, which amounted 50% reduction of the deposit without EMF treatment. However, at 80 °C no deposition was found in the presence of EMF on aluminum surface, comparing to 0.2 mg/cm<sup>2</sup> deposited amount without EMF<sup>117</sup>.

**Anti-scalant.** Anti-scalant is the most commonly used scale inhibition chemicals in water systems, which is considered to be more efficient than EMF on scaling control. Anti-scalants are chemicals such as organophosphonate, polyphosphate- or acidic polymers like polyacrylic acid<sup>118,119</sup>. Corbett<sup>57</sup> reported that EMF was invalid in preventing  $\text{CaSO}_4$  scaling at 91% water recovery in RO system, while the application of anti-scalant sodium hexametaphosphate was successful in avoiding scale at 93% water recovery. Besides, the performance of EMF was compared to the performance of four commercial anti-scalants in retarding the scaling deposition<sup>50</sup>. It was concluded that anti-scalant was scale selective because the anti-scalants of organophosphonate, polymaleic and polyacrylate copolymers had strong resistance on  $\text{CaCO}_3$  and  $\text{CaSO}_4$  scaling but no impact on  $\text{BaSO}_4$  scaling. The other anti-scalant with high specific gravity worked at the opposite way. Although no study combined EMF with anti-scalant in available literature, it can be hypothesized that addition of anti-scalant affect negatively the effectiveness of EMF because their mechanisms for scaling control are conflicting to each other.

## QUANTITATIVE EVALUATION OF EMF IMPROVEMENT

Despite numerous researches have investigated the application of EMF into heat exchangers (Table 1), pipes and other substances (Table 2), bulk solutions (Table 3), membrane systems (Table 4), very few of them have quantified EMF improvement, not to mention the comparison of EMF improvement in the previous review papers<sup>7–9,11,40,99,120</sup>. There are various indicators for different foreign surfaces to evaluate the EMF improvement.



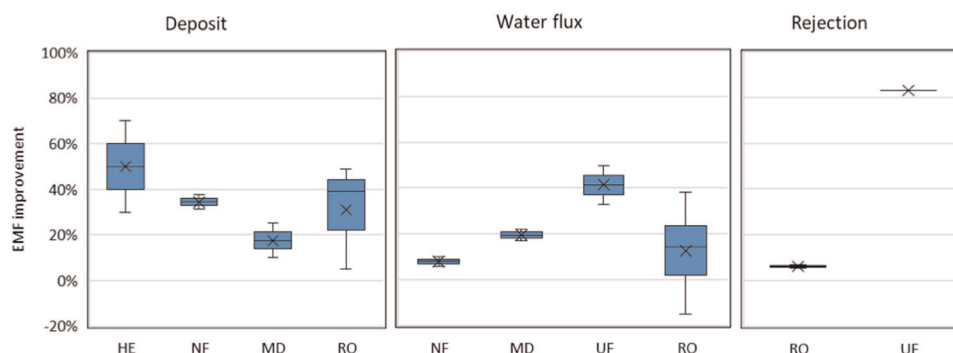


**Fig. 4** Quantification of EMF improvement in terms of scale deposits, water flux, and salt/organic rejection. HE: heat exchanger; NF: nanofiltration; MD: membrane distillation; UF: ultrafiltration; RO: reverse osmosis. The whiskers are the range of the data, the boxes indicate the results of quartile calculation, the crosses are the mean markers.

Because this review focuses on scaling control, scale deposit on the foreign surface, water flux, water recovery, as well as salt/organic rejection were selected as the indicators to evaluate the efficiency of EMF for different water systems. Therefore, this present review has quantified and compared the EMF improvement based on available literature data. The EMF improvement is defined as

$$\begin{aligned} \text{EMF improvement \%} &= \frac{\text{scale deposit without EMF} - \text{scale deposit with EMF}}{\text{scale deposit without EMF}} \times 100\% \quad (\text{for foreign surfaces}) \\ \text{or} &= \frac{\text{water flux with EMF} - \text{water flux without EMF}}{\text{water flux without EMF}} \times 100\% \quad (\text{for membrane systems}) \\ \text{or} &= \frac{\text{salt/organic rejection with EMF} - \text{salt/organic rejection without EMF}}{\text{salt/organic rejection without EMF}} \\ &\times 100\% \quad (\text{for membrane systems}). \end{aligned}$$

Figure 4 summarizes the quantification of EMF improvement in heat exchanger and membrane systems. EMF had positive effect on reducing scale deposit on the heat exchanger<sup>17,42</sup>, NF<sup>53</sup>, MD<sup>54</sup>, and RO systems<sup>51,52,58</sup>. Heat exchanger had the highest improvement<sup>17,42</sup>, implying the efficiency of EMF may relate to temperature. The scale deposit on RO membrane mitigated by 5–49% in different lab-scale and pilot-scale RO systems owing to the variation of feed water and operation parameters<sup>51,58</sup>. EMF enhanced water flux of various membrane systems (Fig. 4). It is worth noting that the negative EMF improvement (–15%) of water flux in RO system came from the water treatment without cartridge filter as pretreatment<sup>58</sup>. Whereas, 17% improvement of EMF treatment was obtained if involved pre-cartridge filters, suggesting the presence of larger particles (>5 µm) in feed water can recede the EMF performance<sup>82</sup>. Moreover, according to the pore size of the testing membranes, the success of EMF may desire larger pore size. There was only 5–7% improvement for salt rejection in RO systems with the application of EMF<sup>52</sup>, thus EMF has marginal effect on salt rejection. Yet, 83% enhancement of organic rejection was achieved in UF system because of coupling electrocoagulation<sup>55</sup>. Pelekani et al. applied pulsed-power EMF into semi-pilot-scale spiral wound RO membrane and found the required time for chemical cleaning of RO system was extended by 33%–49%<sup>51</sup>. However, another research showed EMF was ineffective when installed in a RO desalting plant, significant CaSO<sub>4</sub> scaling was generated on feed spacer and the water recovery decline accelerated approximately 3 times compared to control experiment<sup>57</sup>.

Most studies on operating parameters of EMF applications were limited to laboratory scale with total precipitation or bulk precipitation data only (Tables 1–4). Few researches provided both total precipitation and bulk precipitation<sup>44,46,104,117</sup>, the scale deposit on the pipe or plate surface can be estimated through subtracting bulk precipitation from total precipitation.

Quantification of EMF improvement with different operating parameters is presented in Fig. 5. EMF played a better role on anti-scaling in slightly alkaline solution<sup>44,46</sup>. EMF seemed to have neutral or negative impact on anti-scaling with lower flow rates (0.2–0.4 m/s)<sup>44,46,104</sup>, while the performance of EMF was better at higher flow rate (0.5–1.3 m/s)<sup>110</sup>. EMF reduced the deposition of precipitated CaCO<sub>3</sub> on plate surfaces at a wide temperature range of 20–80 °C. A growth of improvement was observed with increasing temperature, although reproducibility of the experiments at higher temperature (60–80 °C) was poor probably due to the metal surface corrosion (especially of aluminum and copper)<sup>117</sup>. Significant variation in different pH, flow rates, and temperatures was resulted from the difference of pipe/plate materials. As shown in Fig. 5, the application of EMF alleviated the scale adherent in glass and metal (stainless steel, copper, aluminum) surfaces, but aggravated scaling in plastic pipes such as Tygon and PTFE<sup>44,46,104,117</sup>. The effects of materials may contribute to the roughness as glass and metal pipes have smoother surfaces.

## ECONOMIC ANALYSIS

In order to prevent scale formation, conventional chemical treatment technologies have been intensively implemented with considerable consumption of scale inhibition chemicals. EMF could reduce the cost related to chemicals, operation and maintenance. The potential economic benefits of EMF are estimated by comparison with conventional treatment approaches.

Conventional methods of preventing scale formation can be broadly divided into three categories: (i) utilization of scale inhibitors; (ii) system cleaning; (iii) low water recovery for membrane systems<sup>11</sup>. System cleaning such as hydraulic flush and acid cleaning increases the energy, water, and chemical consumption. Operation at low recovery for membrane systems allows the concentration of scale forming ions to be limited to a certain level where precipitation starts<sup>118,121</sup>. However, operation at low water recovery increases treatment cost due to low efficiency and waste of water and energy. Thus, scale inhibitors, including anti-scalant and acid, are required if operating at higher water recovery in membrane systems, and they are the commonly used approaches to mitigate scaling in pipes and heat exchangers<sup>120</sup>. The recommended anti-scalant dosage by manufacturers is commonly below 10 mg/L, with typical range of 0.5–5 mg/L in RO applications. It is because these anti-scalants can serve as a source of nutrients, carbon, and trace elements, which promote biofilm growth<sup>120,122</sup>. Acid injection (i.e., sulfuric acid) to reduce feed solution pH in combination of anti-scalant dosing is of necessity in many cases. The unit weight cost of acid is only a

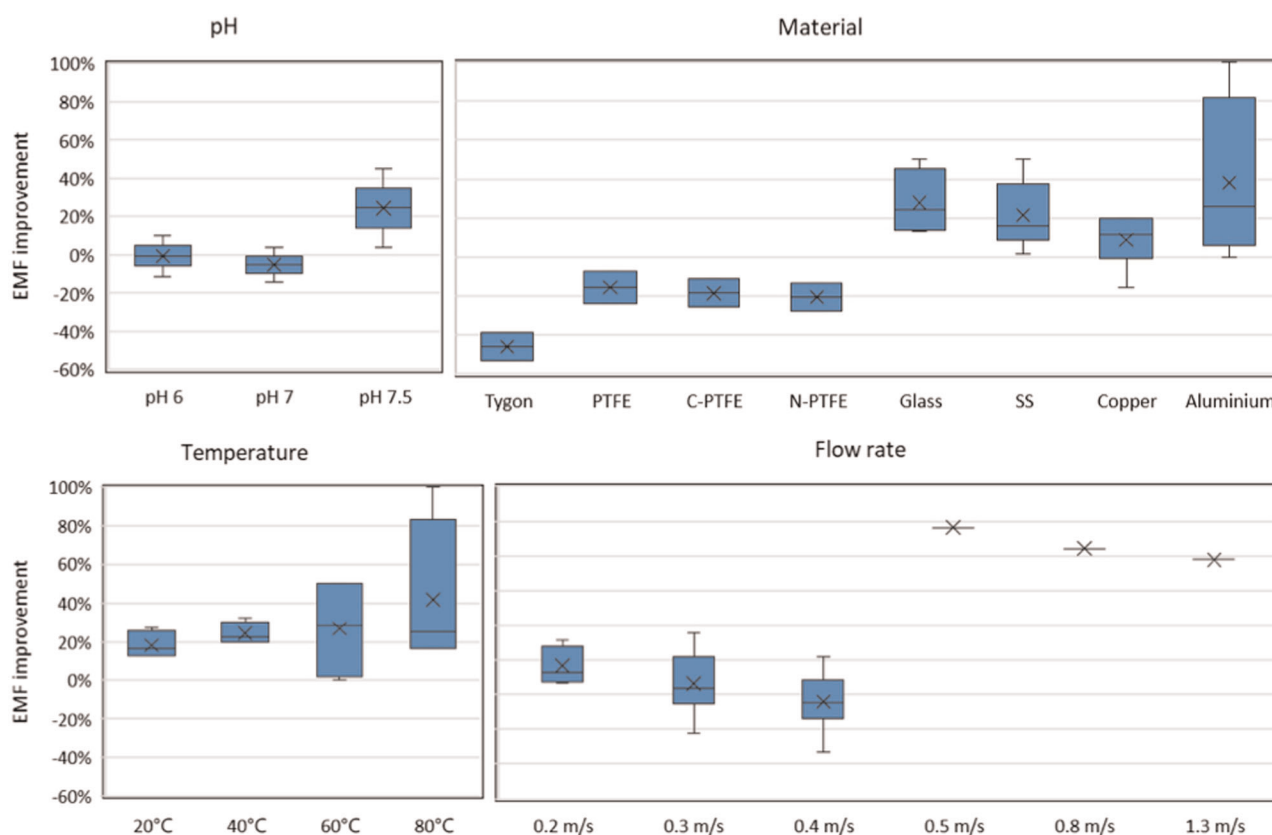


**Fig. 5** Quantification of EMF improvement in terms of scale deposit on the foreign walls. SS: stainless steel; C-PTFE: conductive PTFE; N-PTFE: non-conductive PTFE. The whiskers are the range of the data, the boxes indicate the results of quartile calculation, the crosses are the mean markers.

fraction of that of anti-scalant, while it cannot be neglected considering the enormous dosing volume in large-scale systems, especially in treating water with high alkalinity. The combined costs of pH reduction and anti-scalant are considered as chemical cost. Chemical dosing of acid and anti-scalant for scale control is mostly included in large-scale RO systems, and acid cost could possibly several times higher than the cost of anti-scalant with the fluctuating market price of acid supply<sup>123</sup>. For instance, the 265,000 m<sup>3</sup>/day MF/RO plant of wastewater reuse in Los Angeles had \$0.71 million annual cost for sulfuric acid at pH 7, while increased to \$1.13 million for pH 6 in year 2005. In 2008, the soaring pricing of sulfuric acid increased the acid cost to \$1.97 million and \$10.4 million at pH 7 and 6, respectively. The annual costs of different proposed anti-scalant was maintained below \$1 million.

Moreover, cost of chemical storage, transport, addition and monitoring system, and extra man-hours of maintenance and training (e.g., safety of proper handling chemicals) contributed to other operating cost. Without proper control of scale formation, frequent and aggressive cleaning and/or replacing the failed components, the increased energy input to maintain production or service, or even shutdown, can be a substantial expense. As a non-chemical water treatment technology, EMF can avoid the problems and operating concerns in conventional chemical treatment. An RO plant incorporated with turbulence-promoting distributors and EMF achieved 13% capital cost and 18% energy saving as compared to the traditional ones<sup>124</sup>. More than 20% reduction of transmembrane pressure was observed with 30% reduction of down time on account of saving in membrane cleaning. A pilot comparison of chemical treatment over an EMF

process using electric pulses and DC electric field for cooling towers was conducted at several facilities in California. More than 40% of total cost reduction was observed using EMF process with \$104,067, contrast to \$187,475 using chemical treatment of a cooling tower<sup>125</sup>. Kitman et al. demonstrated that the EMF treatment (using pulsed power) can run 6–8 cycles of concentration in cooling water system, compared to typical 3–5 cycles using the conventional treatment, revealing increased significant annual cost reduction as increasing the size of cooling system (>2500 gallons)<sup>126</sup>.

## CONCLUSIONS AND FUTURE PERSPECTIVES

In the present review, we collected and studied the relevant literature targeting the challenge of scaling control in various water systems, including membranes, heat exchanger systems (e.g. cooling towers), pipes, and bulk solutions, then discussed a number of effects and factors pertaining to EMF water treatment and its anti-scaling effects. According to the more recent and acceptable results from the peer-reviewed scientific works collected in this review, it can be concluded that EMF facilitates bulk precipitation of crystals rather than adhesion to the wall of pipes and vessels. This conclusion is true for majority of the studies at laboratory-, pilot-, and full-scale experiments. However, some studies observed EMF resulted in no difference or negative impacts, probably attributing to the use of non-standardized methods, pipe materials, variations in water chemistry or differences in the course of the treatment.

The scaling prevention mechanisms of EMF can be summarized as hydration effects and magnetohydrodynamic phenomena,

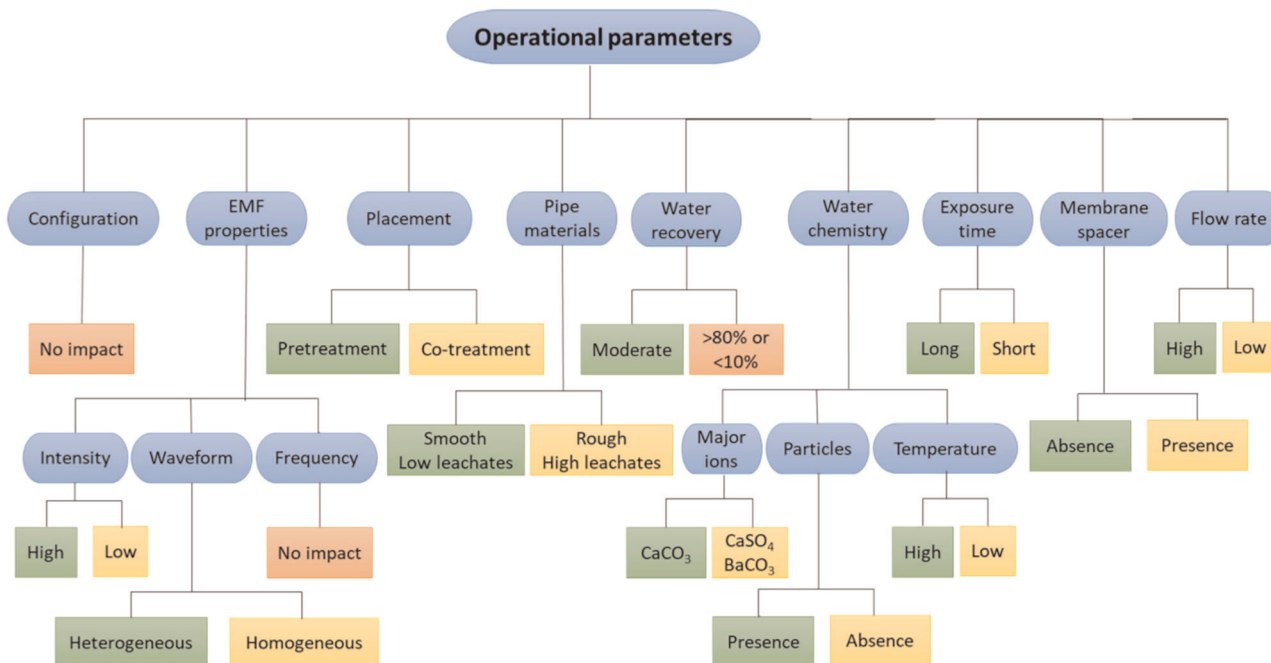


**Fig. 6 Impact of operational parameters on EMF treatment efficiency.** Green box represents positive effect; yellow box represents unclear effect; beige box represents negative or no effect.

which can explain a wide variety of EMF effects. The conventional characterization methods of EMF anti-scaling tests are the weight of precipitates, the remaining concentration of ionic calcium, XRD, SEM, TEM, and EDX. Current real-time monitoring techniques include water/permeate flux, salt rejection, electrochemical tests, surface tension measurement, and optical instrument analysis. Potential real-time monitor techniques were also provided for future application in EMF study.

Based on the comparisons and discussions of EMF effects in the relevant literature, the impacts of operational parameter on EMF treatment efficiency are summarized in Fig. 6, and the primary findings are as following:

- EMF device configuration is not a primary factor for EMF efficiency.
- Higher EMF intensity and less homogeneous waveform contributed to less scaling, negligible effect of frequency was observed.
- EMF as a pretreatment of tested solution raised the anti-scaling efficiency, but different results were obtained when an EMF device placed directly on the scaling surface (co-treatment), probably related to RO system operational conditions.
- Precipitates usually scaled on membrane spacer or block the concentrate flow channel if water recovery is higher than 80%; moderate water recovery is the key factor for successful EMF application.
- The precipitation decreased, and less stable phase of scale was generated as increasing EMF exposure time.
- The impact of pipe material was complex, might be related to roughness of the material and leachate concentration; the total and the bulk precipitation increased simultaneously with roughness of the pipe.
- Higher flow rate improved bulk precipitation, but there is a maximum efficiency for an optimal water flow.
- The effect of EMF was proven to be selective depending on the type of scale: most EMF studies focused on  $\text{CaCO}_3$  and obtained positive results, while different effects of EMF were found on the membrane systems and bulk solutions when the

primary precipitate is  $\text{CaSO}_4$  and  $\text{BaSO}_4$ , probably due to the presence of spacer.

- The presence of suspended particles such as silica is necessary for EMF water treatment to be effective, which can adsorb metal ions and increase bulk precipitation.
- A slight change in pH could affect the precipitation, and the impact of EMF on homogeneous precipitation was more remarkable at lower pH.
- Various experiments implied that EMF had better performance in anti-scaling at higher temperature ( $>70^\circ\text{C}$ ).
- The addition of anti-scalant is more efficient than EMF for membrane scaling control in membrane systems.

For future application, EMF with high intensity and less homogeneous waveform is recommended as a pretreatment for water systems. Longer exposure time and higher flow rate can enhance bulk precipitation. To reduce adherent scaling on the reactor surface, smooth surface and low leachate pipe materials such as glass and metal are recommended. Besides, moderate water recovery ( $<80\%$ ) for RO operation can avoid block of concentrate flow channel. Conventional RO spacer is an obstruct for success of EMF, a new open channel spacer will be advantageous to wash out bulk precipitates and enhance EMF efficiency.

The EMF improvement was quantified and compared based on available literature data. The potential economic savings of the EMF was also reviewed in the present work. This review could establish a series of standard operational parameters and enhance the application or interest for scaling control in large-scale water systems. Hence, additional reproducible studies are required to explore and elucidate the fundamental scientific basis for scaling prevention effects of EMF technologies. To better understand anti-scaling mechanisms, real-time monitoring techniques are needed to apply into EMF treatment systems.

#### DATA AVAILABILITY

The authors declare that all data supporting the findings of this study are available within the paper.

Received: 13 October 2019; Accepted: 24 April 2020;  
Published online: 01 June 2020

## REFERENCES

- Gabrielli, C., Jaouhari, R., Maurin, G. & Keddari, M. Magnetic water treatment for scale prevention. *Water Res.* **35**, 3249–3259 (2001).
- Čolić, M., Chien, A. & Morse, D. Synergistic application of chemical and electromagnetic water treatment in corrosion and scale prevention. *Croat. Chem. Acta* **71**, 905–916 (1998).
- Xu, P. et al. Critical review of desalination concentrate management, treatment and beneficial use. *Environ. Eng. Sci.* **30**, 502–514 (2013).
- Xu, X. et al. Use of drinking water treatment solids for arsenate removal from desalination concentrate. *J. Colloid Interf. Sci.* **445**, 252–261 (2015).
- Lin, L., Xu, X., Papelis, C. & Xu, P. Innovative use of drinking water treatment solids for heavy metals removal from desalination concentrate: Synergistic effect of salts and natural organic matter. *Chem. Eng. Res. Des.* **120**, 231–239 (2017).
- Lin, L., Xu, X., Papelis, C., Cath, T. Y. & Xu, P. Sorption of metals and metalloids from reverse osmosis concentrate on drinking water treatment solids. *Sep. Purif. Technol.* **134**, 37–45 (2014).
- Alabi, A., Chiesa, M., Garlisi, C. & Palmisano, G. Advances in anti-scale magnetic water treatment. *Environ. Sci.: Water Res. Technol.* **1**, 408–425 (2015).
- Baker, J. S. & Judd, S. J. Magnetic amelioration of scale formation. *Water Res.* **30**, 247–260 (1996).
- Antony, A. et al. Scale formation and control in high pressure membrane water treatment systems: a review. *J. Membr. Sci.* **383**, 1–16 (2011).
- Patel, S. & Finan, M. A. New antifoulants for deposit control in MSF and MED plants. *Desalination* **124**, 63–74 (1999).
- Piyadasa, C. et al. The application of electromagnetic fields to the control of the scaling and biofouling of reverse osmosis membranes—a review. *Desalination* **418**, 19–34 (2017).
- Colic, M. & Morse, D. Effects of amplitude of the radiofrequency electromagnetic radiation on aqueous suspensions and solutions. *J. Colloid Interf. Sci.* **200**, 265–272 (1998).
- Amjad, Z. Scale inhibition in desalination applications: an overview. *Corrosion, NACE* **96**–230 (1996).
- Plummer, L. N. & Busenberg, E. The solubilities of calcite, aragonite and vaterite in CO<sub>2</sub>-H<sub>2</sub>O solutions between 0 and 90 °C, and an evaluation of the aqueous model for the system CaCO<sub>3</sub>-CO<sub>2</sub>-H<sub>2</sub>O. *Geochim. Cosmochim. Acta* **46**, 1011–1040 (1982).
- de Leeuw, N. H. & Parker, S. C. Surface structure and morphology of calcium carbonate polymorphs calcite, aragonite, and vaterite: an atomistic approach. *J. Phys. Chem. B* **102**, 2914–2922 (1998).
- Xing, X., Ma, C. & Chen, Y. Investigation on the electromagnetic anti-fouling technology for scale prevention. *Chem. Eng. Technol.* **28**, 1540–1545 (2005).
- Kobe, S., Dražić, G., McGuinness, P. J. & Stražičar, J. The influence of the magnetic field on the crystallisation form of calcium carbonate and the testing of a magnetic water-treatment device. *J. Magn. Magn. Mater.* **236**, 71–76 (2001).
- Knez, S. & Pohar, C. The magnetic field influence on the polymorph composition of CaCO<sub>3</sub> precipitated from carbonized aqueous solutions. *J. Colloid Interf. Sci.* **281**, 377–388 (2005).
- Coey, J. & Cass, S. Magnetic water treatment. *J. Magn. Magn. Mater.* **209**, 71–74 (2000).
- Hater, W. et al. Silica scaling on reverse osmosis membranes—investigation and new test methods. *Desalin. Water Treat.* **31**, 326–330 (2011).
- Bremere, I. et al. Prevention of silica scale in membrane systems: removal of monomer and polymer silica. *Desalination* **132**, 89–100 (2000).
- Demopoulos, G. Aqueous precipitation and crystallization for the production of particulate solids with desired properties. *Hydrometallurgy* **96**, 199–214 (2009).
- Chen, T., Neville, A. & Yuan, M. Calcium carbonate scale formation—assessing the initial stages of precipitation and deposition. *J. Petrol. Sci. Eng.* **46**, 185–194 (2005).
- Mullin, J. *Butterworth Heinemann* (London, UK Oxford, 2001).
- Youngquist, G. R. & Randolph, A. D. Secondary nucleation in a class II system: ammonium sulfate-water. *AIChE J.* **18**, 421–429 (1972).
- Lee, S. & Lee, C.-H. Effect of operating conditions on CaSO<sub>4</sub> scale formation mechanism in nanofiltration for water softening. *Water Res.* **34**, 3854–3866 (2000).
- Lee, S., Kim, J. & Lee, C.-H. Analysis of CaSO<sub>4</sub> scale formation mechanism in various nanofiltration modules. *J. Membr. Sci.* **163**, 63–74 (1999).
- Avlonitis, S., Kouroumbas, K. & Vlachakis, N. Energy consumption and membrane replacement cost for seawater RO desalination plants. *Desalination* **157**, 151–158 (2003).
- Broekman, S., Pohlmann, O., Beardwood, E. & de Meulenaar, E. C. Ultrasonic treatment for microbiological control of water systems. *Ultrason. Sonochem.* **17**, 1041–1048 (2010).
- Coetzee, P., Yacoby, M., Howell, S. & Mubenga, S. Scale reduction and scale modification effects induced by Zn and other metal species in physical water treatment. *Water SA* **24**, 77–84 (1998).
- Tijing, L. D. et al. Mitigation of scaling in heat exchangers by physical water treatment using zinc and tourmaline. *Appl. Therm. Eng.* **31**, 2025–2031 (2011).
- Hou, D., Zhang, L., Fan, H., Wang, J. & Huang, H. Ultrasonic irradiation control of silica fouling during membrane distillation process. *Desalination* **386**, 48–57 (2016).
- Lipus, L. C., Aćko, B. & Hamler, A. Electromagnets for high-flow water processing. *Chem. Eng. Process.* **50**, 952–958 (2011).
- Vallée, P., Lafait, J., Mentré, P., Monod, M.-O. & Thomas, Y. Effects of pulsed low frequency electromagnetic fields on water using photoluminescence spectroscopy: role of bubble/water interface. *J. Chem. Phys.* **122**, 114513 (2005).
- Koza, J. A. et al. Hydrogen evolution under the influence of a magnetic field. *Electrochim. Acta* **56**, 2665–2675 (2011).
- Porter, A. F. Preventing incrustation of steam boilers. U.S. Patent 50,774 (1865).
- A. Faunce, S. C. Electric means for preventing boiler incrustation. U.S. Patent 438,579 (1890).
- Hay, A. T. Electrical protection for boilers. U.S. Patent 140,196 (1873).
- Salman, M., Safar, M. & Al-Nuwaibit, G. The effect of magnetic treatment on retarding scaling deposition. *TOJSAT* **5**, 62–67 (2015).
- Ambashta, R. D. & Sillanpää, M. Water purification using magnetic assistance: a review. *J. Hazard. Mater.* **180**, 38–49 (2010).
- Baker, J. S., Judd, S. J. & Parsons, S. A. Antiscalant magnetic pretreatment of reverse osmosis feedwater. *Desalination* **110**, 151–165 (1997).
- Lipus, L. C. & Dobersek, D. Influence of magnetic field on the aragonite precipitation. *Chem. Eng. Sci.* **62**, 2089–2095 (2007).
- Cho, Y. I., Lane, J. & Kim, W. Pulsed-power treatment for physical water treatment. *Int. Commun. Heat. Mass* **32**, 861–871 (2005).
- Alimi, F., Tlili, M. M., Amor, M. B., Maurin, G. & Gabrielli, C. Effect of magnetic water treatment on calcium carbonate precipitation: Influence of the pipe material. *Chem. Eng. Process.* **48**, 1327–1332 (2009).
- Stuyven, B., Vanbutsele, G., Nuyens, J., Vermant, J. & Martens, J. A. Natural suspended particle fragmentation in magnetic scale prevention device. *Chem. Eng. Sci.* **64**, 1904–1906 (2009).
- Alimi, F., Tlili, M., Ben Amor, M., Gabrielli, C. & Maurin, G. Influence of magnetic field on calcium carbonate precipitation. *Desalination* **206**, 163–168 (2007).
- Kney, A. D. & Parsons, S. A. A spectrophotometer-based study of magnetic water treatment: assessment of ionic vs. surface mechanisms. *Water Res.* **40**, 517–524 (2006).
- Saban, K. V., Jini, T. & Varghese, G. Impact of magnetic field on the nucleation and morphology of calcium carbonate crystals. *Cryst. Res. Technol.* **40**, 748–751 (2005).
- Jianguo, W., Yan, F., Xuemeng, Z. & Xiaomei, L. Effects of alternating electromagnetic field on calcium carbonate scaling process. *ICCE, Melbourne, Australia, Springer, Berlin, Heidelberg* (2011).
- Salman, M. A., Al-Nuwaibit, G., Safar, M. & Al-Mesri, A. Performance of physical treatment method and different commercial antiscalants to control scaling deposition in desalination plant. *Desalination* **369**, 18–25 (2015).
- Pelekani, C., Ostarcevic, E., Drikas, M., Patrick, C. & Cook, D. Reverse osmosis desalination: assessment of a novel electromagnetic field for scale control. *IDA World Congress, Singapore, Membrane Res. Environ.* (2005).
- Carnahan, R. P., Barger, M. & Ghiu, S. *Impact of Magnetic Fields on Reverse Osmosis Separation: A Laboratory Study* (Alighr Muslim University, 2005).
- Li, J., Liu, J., Yang, T. & Xiao, C. Quantitative study of the effect of electromagnetic field on scale deposition on nanofiltration membranes via UTDR. *Water Res.* **41**, 4595–4610 (2007).
- Gryta, M. The influence of magnetic water treatment on CaCO<sub>3</sub> scale formation in membrane distillation process. *Sep. Purif. Technol.* **80**, 293–299 (2011).
- Sun, J. et al. Performance and mechanisms of ultrafiltration membrane fouling mitigation by coupling coagulation and applied electric field in a novel electrocoagulation membrane reactor. *Environ. Sci. Technol.* **51**, 8544–8551 (2017).
- Palmer, N. T., Le, H., Harrington, P. & Furukawa, D. An EMF antiscalant system for desalination of Queensland Nickel's wastewater. In *IDA World Congress, Singapore* (2005).
- Corbett, B. E. *Evaluation of Reverse Osmosis Scaling Prevention Devices at High Recovery* 1–35 (US Department of the Interior Report, 2003).



58. Pellegrino, J. Concentrate Stream Modeling, Electromagnetic Effects on Crystallization, and PP MF Membrane Failure Analysis. *US Dep. Inter. Bur. Reclam.* (2014).
59. Busch, K., Busch, M., McAtee, J., Darling, R. & Parker, D. *Evaluation of the Principles of Magnetic Water Treatment* 960 (American Petroleum Institute Publication, 1985).
60. Busch, K. W., Busch, M., Parker, D., Darling, R. & McAtee, J. Jr Studies of a water treatment device that uses magnetic fields. *Corrosion* **42**, 211–221 (1986).
61. Belova, V. Magnetic treatment of water. US Patent (1972).
62. Srebrenik, S., Nadv, S. & Lin, I. Magnetic treatment of water—a theoretical quantum model. *Phys. Sep. Sci. Eng.* **5**, 71–91 (1993).
63. Gamayunov, N. Coagulation of suspensions after magnetic treatment. *J. Appl. Chem. USSR* **56**, 975–982 (1983).
64. Colic, M. & Morse, D. The elusive mechanism of the magnetic ‘memory’ of water. *Colloid Surf. A* **154**, 167–174 (1999).
65. Madsen, H. E. L. Crystallization of calcium carbonate in magnetic field in ordinary and heavy water. *J. Cryst. Growth* **267**, 251–255 (2004).
66. Madsen, H. L. Influence of magnetic field on the precipitation of some inorganic salts. *J. Cryst. Growth* **152**, 94–100 (1995).
67. Feng-Feng, L., Li-Qiang, Z., Yan-An, G., Gan-Zuo, L. & Zhen-He, T. Effect of sodium halide on dynamic surface tension of a cationic surfactant. *Chin. J. Chem.* **23**, 957–962 (2005).
68. Burgos-Cara, A., Putnis, C. V., Rodriguez-Navarro, C. & Ruiz-Agudo, E. Hydration effects on gypsum dissolution revealed by in situ nanoscale atomic force microscopy observations. *Geochim. Cosmochim. Acta* **179**, 110–122 (2016).
69. Cho, Y. I. & Lee, S.-H. Reduction in the surface tension of water due to physical water treatment for fouling control in heat exchangers. *Int. Commun. Heat. Mass* **32**, 1–9 (2005).
70. Pang, X.-F., Deng, B. & Tang, B. Influences of magnetic field on macroscopic properties of water. *Mod. Phys. Lett. B* **26**, 1250069 (2012).
71. Pang, X. & Deng, B. Investigation of changes in properties of water under the action of a magnetic field. *Sci. Chin. Ser. G* **51**, 1621–1632 (2008).
72. Lower, S. K. *Solids in Contact with Natural Waters* 4–18 (Simon Fraser University, 1997).
73. Vold, R. D. & Vold, M. J. *Colloid and Interface Chemistry* (Addison-Wesley, 1983).
74. Chang, K.-T. & Weng, C.-I. The effect of an external magnetic field on the structure of liquid water using molecular dynamics simulation. *J. Appl. Phys.* **100**, 043917 (2006).
75. Hosoda, H., Mori, H., Sogoshi, N., Nagasawa, A. & Nakabayashi, S. Refractive indices of water and aqueous electrolyte solutions under high magnetic fields. *J. Phys. Chem. A* **108**, 1461–1464 (2004).
76. Amiri, M. & Dadkhah, A. A. On reduction in the surface tension of water due to magnetic treatment. *Colloid Surf. A* **278**, 252–255 (2006).
77. Busch, K. W., Gopalakrishnan, S., Busch, M. A. & Tombácz, E. Magnetohydrodynamic aggregation of cholesterol and polystyrene latex suspensions. *J. Colloid Interf. Sci.* **183**, 528–538 (1996).
78. Rouina, M., Kariminia, H.-R., Mousavi, S. A. & Shahryari, E. Effect of electromagnetic field on membrane fouling in reverse osmosis process. *Desalination* **395**, 41–45 (2016).
79. Stuyven, B. et al. Magnetic field assisted nanoparticle dispersion. *Chem. Commun. (Camb.)*, **2009**, 47–49 (2009).
80. Zhang, Z., Greenberg, A., Krantz, W. & Chai, G. Study of membrane fouling and cleaning in spiral wound modules using ultrasonic time-domain reflectometry. *Membr. Sci. Technol.* **8**, 65–88 (2003).
81. Li, J. & Sanderson, R. In situ measurement of particle deposition and its removal in microfiltration by ultrasonic time-domain reflectometry. *Desalination* **146**, 169–175 (2002).
82. Mairal, A. P., Greenberg, A. R. & Krantz, W. B. Investigation of membrane fouling and cleaning using ultrasonic time-domain reflectometry. *Desalination* **130**, 45–60 (2000).
83. Mairal, A. P., Greenberg, A. R., Krantz, W. B. & Bond, L. J. Real-time measurement of inorganic fouling of RO desalination membranes using ultrasonic time-domain reflectometry. *J. Membr. Sci.* **159**, 185–196 (1999).
84. Li, J., Koen, L., Hallbauer, D., Lorenzen, L. & Sanderson, R. Interpretation of calcium sulfate deposition on reverse osmosis membranes using ultrasonic measurements and a simplified model. *Desalination* **186**, 227–241 (2005).
85. Li, J., Hallbauer, D. & Sanderson, R. Direct monitoring of membrane fouling and cleaning during ultrafiltration using a non-invasive ultrasonic technique. *J. Membr. Sci.* **215**, 33–52 (2003).
86. Chen, J. C., Li, Q. & Elimelech, M. In situ monitoring techniques for concentration polarization and fouling phenomena in membrane filtration. *Adv. Colloid Interf. Sci.* **107**, 83–108 (2004).
87. Uchymiak, M., Rahardianto, A., Lyster, E., Glater, J. & Cohen, Y. A novel RO ex situ scale observation detector (EXSOD) for mineral scale characterization and early detection. *J. Membr. Sci.* **291**, 86–95 (2007).
88. Hickenbottom, K. L. & Cath, T. Y. Sustainable operation of membrane distillation for enhancement of mineral recovery from hypersaline solutions. *J. Membr. Sci.* **454**, 426–435 (2014).
89. Uchymiak, M., Lyster, E., Glater, J. & Cohen, Y. Kinetics of gypsum crystal growth on a reverse osmosis membrane. *J. Membr. Sci.* **314**, 163–172 (2008).
90. Uchymiak, M. et al. Brackish water reverse osmosis (BWRO) operation in feed flow reversal mode using an ex situ scale observation detector (EXSOD). *J. Membr. Sci.* **341**, 60–66 (2009).
91. Gong, J. & Wu, N. *Electric-field Assisted Coating of Nanoparticles for Photon Management Nanostructures* (ACS, Washington, DC, 2015).
92. Antony, A., Chilcott, T., Coster, H. & Leslie, G. In situ structural and functional characterization of reverse osmosis membranes using electrical impedance spectroscopy. *J. Membr. Sci.* **425–426**, 89–97 (2013).
93. Gao, Y. et al. Characterization of forward osmosis membranes by electrochemical impedance spectroscopy. *Desalination* **312**, 45–51 (2013).
94. Sim, L. N., Wang, Z. J., Gu, J., Coster, H. G. L. & Fane, A. G. Detection of reverse osmosis membrane fouling with silica, bovine serum albumin and their mixture using in-situ electrical impedance spectroscopy. *J. Membr. Sci.* **443**, 45–53 (2013).
95. Kavanagh, J. M., Hussain, S., Chilcott, T. C. & Coster, H. G. L. Fouling of reverse osmosis membranes using electrical impedance spectroscopy: measurements and simulations. *Desalination* **236**, 187–193 (2009).
96. Sim, L. N., Gu, J., Coster, H. G. L. & Fane, A. G. Quantitative determination of the electrical properties of RO membranes during fouling and cleaning processes using electrical impedance spectroscopy. *Desalination* **379**, 126–136 (2016).
97. Li, X., Yao, K., Liu, H. & Liu, Z. The investigation of capture behaviors of different shape magnetic sources in the high-gradient magnetic field. *J. Magn. Magn. Mater.* **311**, 481–488 (2007).
98. Britcher, C. P. & Ghofrani, M. A magnetic suspension system with a large angular range. *Rev. Sci. Instrum.* **64**, 1910–1917 (1993).
99. Huchler, L. A., Mar P. E., & Lawrenceville N. J. Non-chemical water treatment systems: histories, principles and literature review. *Int. Water Conf., Pittsburgh*, 02–45 (2002).
100. Tai, C. Y., Yao, C.-K. & Chang, M.-C. Effects of magnetic field on the crystallization of CaCO<sub>3</sub> using permanent magnets. *Chem. Eng. Sci.* **63**, 5606–5612 (2008).
101. Kobe, S. et al. Control over nanocrystallization in turbulent flow in the presence of magnetic fields. *Mater. Sci. Eng.* **23**, 811–815 (2003).
102. Piyadasa, C. et al. The influence of electromagnetic fields from two commercially available water-treatment devices on calcium carbonate precipitation. *Environ. Sci.* **3**, 566–572 (2017).
103. Stojiljković, D. T. et al. Effect of variable frequency electromagnetic field on deposit formation in installations with geothermal water in Sijarinska spa (Serbia). *Therm. Sci.* **15**, 643–648 (2011).
104. Fathi, A., Mohamed, T., Claude, G., Maurin, G. & Mohamed, B. A. Effect of a magnetic water treatment on homogeneous and heterogeneous precipitation of calcium carbonate. *Water Res.* **40**, 1941–1950 (2006).
105. Rizzuti, A. & Leonelli, C. Crystallization of aragonite particles from solution under microwave irradiation. *Powder Technol.* **186**, 255–262 (2008).
106. Junk, G. A., Svec, H. J., Vick, R. D. & Avery, M. J. Contamination of water by synthetic polymer tubes. *Environ. Sci. Technol.* **8**, 1100–1106 (1974).
107. Parker, L. V. & Ranney, T. A. Sampling trace-level organic solutes with polymeric tubing: I. Static studies. *Groundw. Monit. Remediat.* **17**, 115–124 (1997).
108. Shockling, M., Allen, J. & Smits, A. Roughness effects in turbulent pipe flow. *J. Fluid Mech.* **564**, 267–285 (2006).
109. Flack, K. A., Schultz, M. P. & Shapiro, T. A. Experimental support for Townsend’s Reynolds number similarity hypothesis on rough walls. *Phys. Fluids* **17**, 035102 (2005).
110. Shahryari, A. & Pakshir, M. Influence of a modulated electromagnetic field on fouling in a double-pipe heat exchanger. *J. Mater. Proces. Technol.* **203**, 389–395 (2008).
111. Landau, L. D. et al. *Electrodynamics of Continuous Media* (Elsevier, 2013).
112. Jiang, W. et al. A pilot study of an electromagnetic field for control of reverse osmosis membrane fouling and scaling during Brackish groundwater desalination. *Water* **11**, 1015 (2019).
113. Szkutala, A., Balanda, M. & Kopeć, M. Magnetic treatment of industrial water. Silica activation. *Eur. Phys. J. Appl. Phys.* **18**, 41–49 (2002).
114. Parsons, S., Judd, S., Stephenson, T., Udol, S. & Wang, B. Magnetically augmented water treatment. *Process Saf. Environ.* **75**, 98–104 (1997).
115. Higashitani, K. & Oshitani, J. Magnetic effects on thickness of adsorbed layer in aqueous solutions evaluated directly by atomic force microscope. *J. Colloid Interf. Sci.* **204**, 363–368 (1998).
116. Higashitani, K., Oshitani, J. & Ohmura, N. Effects of magnetic field on water investigated with fluorescent probes. *Colloids Surf. A* **109**, 167–173 (1996).



117. Chibowski, E., Holysz, L. & Szczes, A. Adhesion of in situ precipitated calcium carbonate in the presence and absence of magnetic field in quiescent conditions on different solid surfaces. *Water Res.* **37**, 4685–4692 (2003).
118. Micale, G., Cipollina, A. & Rizzuti, L. *Seawater Desalination* (Springer, 2009).
119. Greenlee, L. F., Lawler, D. F., Freeman, B. D., Marrot, B. & Moulin, P. Reverse osmosis desalination: Water sources, technology, and today's challenges. *Water Res.* **43**, 2317–2348 (2009).
120. Hasson, D., Shemer, H. & Sher, A. State of the art of friendly “green” scale control inhibitors: a review article. *Ind. Eng. Chem. Res.* **50**, 7601–7607 (2011).
121. Williams, M. E. A *Brief Review of Reverse Osmosis Membrane Technology* (EET Corporation and Williams Engineering Services Company Inc., 2003).
122. Crabtree, M. et al. Fighting scale—removal and prevention. *Oilfield Rev.* **11**, 30–45 (1999).
123. Malki, M. *Case Study: Optimizing Scale Inhibition Costs in Reverse Osmosis Desalination Plants 1–8* (American Water Chemicals, Inc., 2009).
124. Vedavyasan, C. Pontential use of magnetic fields—a perspective. *Desalination* **134**, 105–108 (2001).
125. Technology, O. O. P. P. A. G. *Evaluation of Non-Chemical Treatment Technologies for Cooling Towers at Select California Facilities 1–57* (California Department of Toxic Substances Control, 2009).
126. Kitman, K. A., Maziarz, E. F., Padgett, B., Blumenschein, C. D. & Smith, A. Chemical vs. non-chemical cooling water treatments—a side-by-side comparison. *IWC* **3**, 22 (2003).
127. Xing, X.-k, Ma, C.-f, Chen, Y.-c, Wu, Z.-h & Wang, X.-r Electromagnetic anti-fouling technology for prevention of scale. *J. Cent. South Univ. Technol.* **13**, 68–74 (2006).
128. Xuefei, M., Lan, X., Jiapeng, C., Zikang, Y. & Wei, H. Experimental study on calcium carbonate precipitation using electromagnetic field treatment. *Water Sci. Technol.* **67**, 2784–2790 (2013).
129. Zhao, J.-D., Liu, Z.-A. & Zhao, E.-J. Combined effect of constant high voltage electrostatic field and variable frequency pulsed electromagnetic field on the morphology of calcium carbonate scale in circulating cooling water systems. *Water Sci. Technol.* **70**, 1074–1082 (2014).
130. Al Helal, A., Soames, A., Gubner, R., Iglaue, S. & Barifcani, A. Influence of magnetic fields on calcium carbonate scaling in aqueous solutions at 150 °C and 1bar. *J. Colloid Interf. Sci.* **509**, 472–484 (2018).
131. Xu, Z., Chang, H., Wang, B., Wang, J. & Zhao, Q. Characteristics of calcium carbonate fouling on heat transfer surfaces under the action of electric fields. *J. Mech. Sci. Technol.* **32**, 3445–3451 (2018).
132. Cefalas, A. C. et al. Nanocrystallization of CaCO<sub>3</sub> at solid/liquid interfaces in magnetic field: a quantum approach. *Appl. Surf. Sci.* **254**, 6715–6724 (2008).
133. Benson, R. F., Lubosco, R. & Martin, D. F. Magnetic treatment of solid carbonates, sulfates, and phosphates of calcium. *J. Environ. Sci. Health* **35**, 1527–1540 (2000).
134. Saksono, N., Yuliusman, Y., Bismo, S., Soemantojo, R. & Manaf, A. Effects of pH on calcium carbonate precipitation under magnetic field. *Makara J. Technol.* **13**, 79–85 (2010).
135. Salman, M. & Al-Nuwaibit, G. Anti-scale magnetic method as a prevention method for calcium carbonate scaling. *TOJSAT* **7**, (2017).
136. Han, Y. et al. Effect of alternating electromagnetic field and ultrasonic on CaCO<sub>3</sub> scale inhibitive performance of EDTMPS. *J. Taiwan Inst. Chem. Eng.* **99**, 104–112 (2019).
137. Han, Y. et al. Influence of alternating electromagnetic field and ultrasonic on calcium carbonate crystallization in the presence of magnesium ions. *J. Cryst. Growth* **499**, 67–76 (2018).
138. Karkush, M. O., Ahmed, M. D. & Al-Ani, S. M. Effects of magnetic fields on the properties of water treated by reversed osmosis. Preprint (2019).

## ACKNOWLEDGEMENTS

Support for this study was provided by the United States National Science Foundation (NSF) Engineering Research Center Program under Cooperative Agreement EEC-1028968 (ReNUWit); and the United States Bureau of Reclamation under Agreement R18AC00118.

## AUTHOR CONTRIBUTIONS

Literature review, data collection and analysis: L. Lin, W. Jiang, X. Xu, and P. Xu; Paper writing—original draft: L. Lin, W. Jiang, X. Xu; Writing—review and editing: L. Lin and P. Xu; Funding acquisition, project administration, and supervision: P. Xu.

## COMPETING INTERESTS

The authors declare no competing interests.

## ADDITIONAL INFORMATION

**Correspondence** and requests for materials should be addressed to P.X.

**Reprints and permission information** is available at <http://www.nature.com/reprints>

**Publisher's note** Springer Nature remains neutral with regard to jurisdictional claims in published maps and institutional affiliations.



**Open Access** This article is licensed under a Creative Commons Attribution 4.0 International License, which permits use, sharing, adaptation, distribution and reproduction in any medium or format, as long as you give appropriate credit to the original author(s) and the source, provide a link to the Creative Commons license, and indicate if changes were made. The images or other third party material in this article are included in the article's Creative Commons license, unless indicated otherwise in a credit line to the material. If material is not included in the article's Creative Commons license and your intended use is not permitted by statutory regulation or exceeds the permitted use, you will need to obtain permission directly from the copyright holder. To view a copy of this license, visit <http://creativecommons.org/licenses/by/4.0/>.

© The Author(s) 2020